Neural Pathways Integrating Circadian Information into the Decision to Trigger Ovulation

Benjamin Smarr

A dissertation

Submitted in partial fulfillment of the

Requirements of the degree of

Doctor of Philosophy

University of Washington

2012

Reading Committee:

Horacio de la Iglesia, Chair

Martha Bosma

Donald Clifton

Program Authorized to Offer Degree:

Neurobiology and Behavior

University of Washington

Abstract

Neural Pathways Integrating Circadian Information into the Decision to Trigger Ovulation

Benjamin Smarr

Dr. Horacio de la Iglesia, Chair

It has long been known that time-of-day information is required for successful initiation of the ovulation-triggering luteinizing hormone (LH) surge. This is true in rodents and evidence suggests it is true in humans too. LH release is driven by neural release of gonadotropin-releasing hormone (GnRH) from GnRH neurons in the medial preoptic area of the hypothalamus, and these neurons represent the last neuronal control point in the brain's decision to ovulate for all vertebrates. Time of day, or circadian, information is centrally regulated by the suprachiasmatic nucleus, also in the hypothalamus. How information from the SCN reaches the GnRH neurons was not known. Female rats are similar to humans in both relevant neurological structure and behavioral and physiological responses to circadian challenges. Using female rats as a model system, I provide evidence here that the suprachiasmatic nucleus times ovulation indirectly through projections from the dorsomedial (dm) SCN to the anteroventral periventricular nucleus (AVPV), wherein kisspeptin-producing neurons integrate this circadian information with estrodiol levels. I further show evidence suggesting that the AVPV is a peripheral circadian oscillator entrained by the dmSCN, and that circadian phase within the AVPV drives its receptivity to vasopressin – the primary neuropeptide transmitter released from the dmSCN. If both hormonal (estradiol) and daily cycles are in the right phase, then kisspeptin neurons stimulate GnRH neurons to trigger the LH surge. Kisspeptin is the strongest known driver of GnRH neuronal excitation, but I demonstrate that GnRH cells still exert some kisspeptin-independent control over the shape of the

LH surge by integrating information coded by the ventrolateral SCN, which influences the amplitude of the LH surge in a phase-dependant manner.

TABLE OF CONTENTS

Page

List of Figures

Forward by the author.

In an effort to aid my readers, I feel I should make explicit some of my basic assumptions about how biology works, so that comments in the following chapters may be taken as I mean them. Life is not special in and of itself. Rather, what we recognize as life can be thought of entirely as a persistent, anti-entropic reaction, and we notice it because of this property. Because entropy increases by law, it follows that anything which not only persists in having structure but actively maintains that structure, must be a) locally and self-perpetuatingly anti-entropic, and therefore b) energetically expensive. The trick with Life is that is has figured out how to fix energy from its surroundings for use in perpetuating local structure (by local I mean the opposite of global/universal). Because entropy always increases globally, any anti-entropic system must be confined locally to where the energy is fixed. Furthermore, complex anti-entropic systems must also maintain structure for energy transfer, which itself requires energy to maintain. Therefore, efficiency of energy allocation must increase with complexity of anti-entropic systems such as life.

Surely any cell hoping to optimize its energy use – and any organism hoping to get optimal function from its cells – will need very complex signaling systems to inform local tissues what state they should be in. Furthermore, we can expect these signaling systems to be shaped in such a way as to optimize energy consumption, within some constraints I will lay out shortly. In this way, I suggest that all of biological organization and function can be thought of as either energy fixation or energy allocation (i.e. information transfer across space), and arguably both.

Evolution arises from the simple facts that maintaining anti-entropic activities is energetically expensive, and that a constant energy supply cannot be guaranteed in a semi-chaotic environment (like ours), meaning the amount of energy available from the environment changes with time, and some of those changes are unpredictable. Therefore systems that are most energetically efficient will have the greatest probability of persisting through time. All adaptations therefore suggest themselves as being in some way energetically favorable for the environment in which they arose, even if only at a population level. This again is because those populations carrying information that increases the probability of survival past episodic losses of available energy in the environment will be more likely to persist than those without this advantage. This does not imply, however, that all entities (e.g. species) within biological evolution have followed the same path towards energetic efficiency.

The chaotic nature of the environment means that different locations and times will have different energetic characteristics. As a result, adaptation will look different in different parts of this energetic landscape. To understand why this causes lineages to arise – why information about the past should inform knowledge of the present – we must think about how these adaptations take place. Radical structural changes would allow for quick adaptation to changes in the environment, but such radical changes are not what we see in biological evolution (lizards do not spontaneously develop wooly coats if an ice-age arises in their vicinity). This is because the larger the change that occurs in a given system with some organizational constraint, the more energetically expensive and therefore improbable such a change becomes. So Life can effectively only optimize its energy efficiency through changes that occur at lower (ambient) energy states (i.e. molecular jostling during DNA replication to

cause mutations is more likely than spontaneous generation of wooly coats). This is of critical importance to understanding why Life is shaped as it is. The energetic limitation on probable change within a given structure implies that at any given moment, a system's structure should be similar to that system's structure in the previous moment. Thus one must look at Life as a self-perpetuating, anti-entropic system becoming more and more efficient in its local environment, but also as a system with a fundamentally limited rate of change. The study of biology must therefore be as much a study of energetics as of history, and fate effectively plays as large a role as thermodynamic principle. As biologists, if we want to understand the structure of a biological system, we must look at the historical energetics of that system's environment so that we may predict how the system was efficient within that history.

The rate of change within a biological system may be much slower – given the constraints on scale of change discussed above – than the semi-chaotic changes in the environment (e.g. an ice age causes extinctions because the rate of environmental change exceeds the rate of biological change to regain efficiency in the new energetic environment). Thus looking only at the current environment of an organism and trying to ascertain how the organism is adapted to that environment is unwise. A wiser approach to unraveling the functions of specific systemic organization in biology would seem to be to understand the environmental forces shaping the historical growth of that structure, and using that knowledge to predict and then search for optimizations based on those historical constraints, or disruptions that might arise from changes in the environment that outstrip the rate of biological optimization to that environment.

For example, as I will discuss in chapter 1, it is energetically efficient to predict the time-of-day-variance-in-available-solar-energy so that energy is not wasted in post-facto responses to what were in fact predictable events. This leads to the evolution of the circadian system. Its genetic clockwork and interconnected signaling are all to provide coordinated information about time (and the information about predictable states which that implies) across cells, organisms, and super-organisms like our society. The driver and result is that energetic efficiency across structural scales (within the local bounds of whatever preexisting state) can be realized. As would be predicted by my hypothesis about loss of efficiency from sudden environmental changes, modern technology – from lighting to 24/7 economic and thereby social drive – has disrupted the circadian environment of modern humans. This dissertation deals with understanding the details behind one result of this – disrupted timing signals to the reproductive axis in females. It also takes advantage of this disruption to reveal fundamental workings of the intact system.

Throughout the following text, references to energy, efficiency, and information are to be taken in the context presented above – that is, that the purpose of a hormone is to signal, which means to convey information, and that the purpose of that information is regulation of specific energy-allocation tasks, like making new receptor proteins. This was probably a long way of saying what is obvious to most readers, but it makes the context of what follows explicit, and I hope less potentially confusing as a result.

On a personal note, I would say I see this thesis less as about circadian biology, or about reproductive biology, than as about behavioral decision-making. Studying how the mammalian

brain renders specific decisions is difficult, especially when those decisions involve social choice and changing cue salience. Such decisions are an every-day matter of course for all of us, and disruptions of the neural mechanisms responsible can cause generally undesirable states, such as depression. Unfortunately for those who seek to understand these neural mechanisms, such behaviors are often viewed as subjective (therefore hard to quantify and trace) and subtle (therefore hard to model and prone to high-variance under subjective measure). Both the circadian and reproductive systems modulate behavioral decisions in profound ways. The circadian system takes mammals from conscious to inert, and the reproductive system from violently antisocial to physically amorous. Both do so predictably in time! That predictability makes these modulators potentially powerful instruments in tracing the neural correlates of mood and behavioral decision-making. This dissertation is, at its core, a proof of concept for using these systems to identify the specific connectivity and conditional variables which represent the physical instantiation of a neural decision with broad behavioral consequences, using the hormonal signal that triggers ovulation as an eminently tractable decision output

Chapter 1: Introduction to Neural Control of Ovulation and Evidence of Circadian Input

The decision made by the mammalian female brain to ovulate is dependent on the integration of information from two different endogenous oscillator systems with different oscillatory periods. The first is the female ovulatory cycle, which in rats has a period of 4-5 days and the phase of which can be marked by the pre-ovulatory surge of luteinizing hormone (LH) in the systemic blood stream. The second oscillatory system is the circadian, or daily, cycle. The phase of this rhythm is most easily measured by onset of daily consolidated bouts of locomotor activity, which can be predicted with a precision within minutes. Loss of either of these oscillations in mature females results in an anovulatory state, and an inability to reproduce[1–7]. Despite the central biological significance of the integration of information between these two systems, the site and nature of this integration is not known. Uncovering it is the focus of this dissertation.

The Female Reproductive Oscillator.

The ovulatory oscillator is created by feedback between three organs – the hypothalamus, pituitary, and ovary. Gonadotropin releasing hormone (GnRH)-containing neurons in the medial preoptic area (MPO) of the hypothalamus release GnRH in pulses into the hypophyseal portal system [8–12] – a capillary bed that perfuses the anterior pituitary, also called the adenohypophysis. There, GnRH stimulates gonadotrophic cells to release LH and follicle stimulating hormone (FSH)[8,10,11,13,14], which travel through the systemic circulation and prime one or more ovarian follicles. The ovary in turn produces hormones, chiefly estradiol (E_2) and progesterone (P), which feedback to the hypothalamus and pituitary, modulating gonadotroph

excitation and gonadotropin release [15–18]. This tissue loop is called the hypothalamo-pituitary-gonadal (HPG) axis.

In rats, the day before ovulation – proestrus – is marked by a rise in E_2. Once E_2 passes a threshold (the mechanism of which remains unclear), it causes GnRH release to increase dramatically. In rats with lesions of the MPO, E_2 replacement is insufficient to stimulate an LH surge, suggesting that the E_2 integrator must be upstream of the gonadotrophs. However GnRH cells lack estrogen receptor alpha (ERα), the ER needed to drive this surge in GnRH release[19–21], suggesting that here E_2 is acting through some neural population upstream of the GnRH cells. The high-E_2-modulated surge in release of GnRH leads to a surge in the release of LH, known as the preovulatory LH surge. The full LH surge is the product of a female-specific feed-forward cycle wherein LH release stimulates further E_2 release from the ovaries, which in turn stimulates further GnRH release and, in turn, LH release[22–25]. This surge stimulates the primed ovarian follicle to rupture, releasing an egg in the act of ovulation[25]. At this point the surge declines, with LH turning the ruptured follicle into the luteal body which promotes P production, and inhibits more E_2 release[25]. The full 4 day ovulatory cycle in rats is called the estrous cycle, as with other animals that do not menstruate. Estrous cycles often immediately follow ovulation with behavioral changes in estrus, such as sudden sexual receptivity in otherwise sexually un-receptive female rats[26,27]. Menstrual cycles can show some behavioral modulation, but it is much less pronounced[28]. The hormonal control in rats and humans, while not exactly the same, appears remarkably similar. However there is considerable debate about specific control mechanism similarities between rodents, primates, and humans. The experiments in this paper focus on the rat, and connections to humans remain suggestive.

The Master Circadian Oscillator.

The circadian oscillator is centralized in the hypothalamic suprachiasmatic nucleus (SCN)[29]. Individual cells within the SCN generate oscillatory output with a circadian period, though individual cells may differ in the exact period[30]. These oscillations are not generated by the emergent properties of large-scale multi-tissue feedback systems as with the HPG axis, but instead by intracellular transcriptional feedback loops wherein gene products feed back to inhibit their own transcription, leading to 24-h oscillations in their mRNA and protein levels[31–34]. Several of these so-called clock genes have been well characterized, and their levels represent phase markers for these intracellular circadian oscillators[35–39]. A number of mutations in clock genes have been discovered, such as the *Tau* mutation, which alters the circadian period (tau) by changing the mutated clock gene product's interaction dynamics[40]. Through mechanisms yet to be fully revealed, single-cell neuronal oscillators within the SCN show strong coupling and oscillate in synchrony as a tissue oscillator[41,42]. In the rat, cells in the ventrolateral (vl) SCN receive glutamatergic input from the retina, which relay light information that can reset vlSCN neuronal oscillators and entrain them to the environmental light-dark (LD) cycle [43–45]. The vlSCN in turn entrains the SCN's dorsomedial (dm) neuronal oscillators, so that the whole tissue remains synchronized. Without this retinal input the SCN "free-runs," oscillating according to its own endogenous period[46,47]. In the rat, the SCN's (and therefore the animal's) free-running period (FRP) is about 24.7 h, though there is variance among strains and individuals.

When removed from its host and kept alive *in vitro*, the SCN persists in circadian expression of clock genes, electrical activity and neurotransmitter release[48,49], while an animal

with a complete SCN lesion becomes arrhythmic [50–53]. Implantation of fetal SCN tissue to the third ventricle restores locomotor activity rhythms in SCN-lesioned animals[54–56]; implantation of a *Tau* mutant SCN (which has an abnormally short ~20h period) into a wild-type SCN-lesioned host restores circadian rhythmicity with the donor-specific period[53]. Though other extra-SCN tissues show circadian oscillations [32,36,48,57–63], none can restore circadian rhythmicity after transplantation. Furthermore, SCN lesions abolish all overt behavioral and physiological circadian rhythms [52,64(p-)]. For this reason the SCN is considered the master circadian pacemaker. Whereas most tissues show autonomous circadian oscillations in clock gene expression which persist in their circadian oscillations after their isolation ex-vivo[32,36(p2),65], the phase of these peripheral oscillators depends on signals from the SCN [64,66,67], which maintain the internal synchronization between all the oscillators in the body. Thus, the master regulation of rhythms by the SCN may in part rely on the regulation of peripheral oscillators that presumably exert local control of physiological rhythms.

Circadian Modulation of the HPG Axis.

In rats in proestrus, the LH surge occurs just before the onset of daily locomotor activity. If endogenous estrogen is controlled by removing the ovaries and administering exogenous E_2, rats show daily afternoon peaks of LH[2]. In ovariectomized, E_2-treated *Tau* mutant hamsters, the LH surge occurs every ~20 h, on schedule with the mutant FRP [68]. When animals are subjected to phase-shifts (as in jet lag), the phase of the LH surge shifts to maintain its relationship with the circadian oscillations [69–72]. When the central oscillator is temporarily slowed by application of heavy water (the mechanism of which remains unclear), the LH surge maintains its phase

relationship to the onset of locomotor activity regardless of the FRP[73]. Finally, lesions of the SCN abolish these daily LH surges [29,74,75], suggesting that the SCN sends an essential circadian triggering signal to the HPG axis.

These and other results have established that the LH surge results from integration of high E_2 levels from the ovaries and a circadian signal from the SCN that converge into the hypothalamus at or downstream from the SCN, but upstream from GnRH cells in the MPO. In rats, mice and hamsters the surge occurs in the evening, beginning 2-3 h before their nocturnal activity onset. In humans, the pre-ovulatory LH surge takes place primarily in the early morning[7677], also preceding daily locomotor activity. Disruption of internal circadian timing by shift-work or jetlag is associated with reproductive disorders[78–80], suggesting that intact circadian regulation of the HPG axis is critical for regular reproductive cycles and ovulation in women. Transplanting a fetal SCN into the third ventricle of SCN-lesioned hosts will restore locomotor rhythmicity but not hormonal rhythmicity[64]. This suggests that the relevant circadian information reaches the HPG axis through specific neuronal projections and synaptic connections. Evidence accumulated over the last 10 years suggests that Kisspeptin, a key regulator of GnRH neurons, may act as a key integrator between the circadian and estrogen cycles.

Kisspeptin and its Regulation of GnRH release.

Kisspeptin (Kiss1, coded by the *Kiss1* gene) is a 54 base pair peptide produced primarily in the arcuate (ARC) and the anteroventral periventricular nucleus (AVPV) of the mammalian hypothalamus[81–88]. Kiss1 was initially discovered in Hershey, PA, and so its name derives from

the locally produced chocolate candy, and not its role as a precursor to successful reproduction. Originally studied as a potential metastatic inhibiting factor, it has become clear that Kiss1 serves a central role in regulating GnRH release both at the MPO and the median eminence – the area at the base of the hypothalamus where nerve terminals release hypothalamic releasing-hormones into the hypophyseal portal blood system. As such, Kiss1 is crucial for regular female reproductive cycles [89].

Application of Kiss1 is the strongest driver of GnRH release yet found; acute central or peripheral application into E_2-primed females causes substantial LH release in rodents, sheep, primates, and humans [81,82,90–94]. Application ex vivo of even nanomolar concentrations to slices containing GnRH cells causes GnRH cells to fire tonic action potentials for up to an hour [95] As already stated, GnRH cells lack ERα. Therefore, the effects of E_2 on GnRH release described above are likely mediated upstream of GnRH cells. $Kiss^+$ cells within the AVPV and the ARC express ERα (Smith et al., 2005), potentially filling this role. However in rodents the ARC seems to be involved in negative feedback from E_2 [96–98], while the AVPV is more likely the site of positive feedback driving the LH surge [6,99–104]

In rodents, E_2 diminishes *Kiss1* expression in the ARC [105,106]. Most ARC cells expressing *Kiss1* also express dynorphin (DYN) and neurokinin B (NKB)[107–109], the latter of which is known to inhibit GnRH release[110]. Colocalization of these peptides within the AVPV is much lower, on the order of 10% [109,111–113]. These ARC KISS cells send projections to GnRH terminals in the median eminence [114–116], and also project extensively to each other [117]. A feedback cycle has been suggested whereby NKB release within the ARC stimulates KISS release, but also DYN,

which inhibits KISS release and NKB release[118]. Such a mechanism could generate the typical pulses of GnRH and LH that persist throughout the reproductive cycle. This has not been proven but it is consistent with work—before the discovery of KISS—by Knobil and collaborators, who found that ablation of the ARC in primates caused a loss of pulsatile GnRH release[119].

Within the AVPV, E_2 stimulates expression of *Kiss1*[105,106], which is sexually dimorphic in the mouse and rat AVPV 106 107 15 50[83,120–122]. Female rodents and primates have higher numbers of *Kiss1*-positive cell bodies than males, and the number of *Kiss1*-expressing cells, as well as the levels of *Kiss1* expression in these cells, increases at the onset of puberty[82,83,91,123]. This expression increases thereafter periodically around the time of ovulation[87,122,124,125]. In mice and rats Kiss1-postitive neurons in the AVPV send axonal fibers proximally to GnRH cell bodies in the MPO [87,126] , and the number of these fibers also increases during puberty [83]. Direct, structural evidence of functional synapses has not been shown, but the Kiss1 receptor Kissr1—formerly known as GPR54 —is highly penetrant across the GnRH cell population responsible for the LH surge in rats and mice [83,127]. Mice and humans lacking a functioning Kiss1r display hypogonadotropic hypogonadism [89,128–131] and blockade of Kiss1 signaling with antisera against Kiss1 blocks the LH surge[124124]. It should be noted that in sheep, primates, and humans, the AVPV population is proportionately smaller than in the mouse or rat [82,84–86], though the significance of this difference is not known. Despite the central importance of Kiss1 in reproduction and its proven role as a driver of GnRH release and the LH surge, little is known about what regulates the synthesis and release of Kiss1 or the activity of its coding gene *Kiss1*.

Potential SCN modulation of KISS.

Rats normally show consolidated bouts of locomotor activity, which match the phase of SCN-clock gene oscillations, which are in turn entrained to the 24h environmental light-dark (LD24) cycle. However, rats exposed to an 11:11 light-dark (LD) cycle (LD22) develop two locomotor activity rhythms with differing periods: one rhythm is entrained to the 22-h LD cycle and the other rhythm is dissociated from it and shows a period of ~25 h. Using male rats, de la Iglesia *et al.* have demonstrated that the 22h-rhythm in the clock gene expression of the vlSCN is associated with the 22h locomotor activity rhythm. In contrast, the LD-dissociated rhythm is associated with a clock-gene expression rhythm within the dmSCN [132]. Work by our lab has previously shown that this ~25h rhythm is not truly free-running, but still weakly coupled to the vlSCN [133]; therefore I will not refer to it as the free-running rhythm. Instead, I will refer to these rhythms as the vlSCN-associated and dmSCN-associated rhythms, under the assumption that each locomotor activity rhythm represents the output of the vl- and dmSCN, respectively. As the two rhythms in the LD22 desynchronized rat come in and out of phase with each other, the animals experience days of alignment, where both activity phases coincide, and days of misalignment, where the activity phase of one rhythm ends as the activity phase of the other begins. The vl- and dmSCN also differ from each other in projection patterns and neurotransmitter profiles [134]. Many cells in the vlSCN produce and signal with vasoactive intestinal poly peptide (VIP), while many cells in the dmSCN produce and signal with arginine-vasopressin (AVP)[134]. VIPergic SCN fibers project directly to GnRH cells in the MPO, while the AVPergic SCN fibers project to ERα-containing neurons in the AVPV [135–137]. Lesions of either the AVPV [99] or the SCN [5,138] abolish the LH surge, suggesting that having an intact SCN and GnRH cell population is still insufficient to drive the LH surge. Taken together, these results have led

to the formulation of the following model: information about estrogen levels, monitored by AVPV ERα-containing cells, converges with input from the SCN circadian information at the level of the AVPV and/or directly on GnRH cells.

The targeted administration of AVP near the AVPV induces LH surges in SCN-lesioned mice [139] and rats [75]. However, there is also evidence that VIP modulates the timing of the LH surge and the activity of GnRH cells in rats [140–143]. The relative influence of VIP and AVP in gating an LH surge remains controversial and its assessment has been complicated by non-specific effects of lesions. Although the precise nature of the SCN signal gating the surge remains to be elucidated, evidence suggests that *Kiss1*-positive cells may be an integrator of this signal. Our lab has shown that in OVX mice with E_2 implants, expression of *Kiss1*, as well as of *c-fos* within *Kiss1*$^+$ cells, showed circadian oscillations with a peak matching the time of the LH surge.

Taken together, these data raise the questions of (1) whether the E_2 and circadian oscillators converge into an integrator within MPO or upstream in the AVPV, (2) which SCN neuronal oscillators and neurotransmitters code for the relevant phase information, and (3) how the integrator site acts as a coincidence detector of hormonal and circadian information to trigger the LH surge. The data in the following chapters seeks to directly address these questions, using the rat as a model organism.

Chapter 2: The Master Circadian Clock is Necessary for Circadian *Kiss1* Expression in the AVPV and Circadian GnRH Cell Activation.

Mice show E_2-dependent *Kiss1* circadian rhythms in the AVPV[125]. I examined expression of *Kiss1* mRNA in OVX rats primed with E_2 (OVX+E_2). Brains collected every 6 h during the first 24 h after their release into constant darkness showed a rhythm with a peak that coincided with the afternoon LH surge (one-way ANOVA for *Kiss1* levels, $F = 0.023$, $p = 0.023$, n = 4-6 per time point) (Fig. 2.1). I then assayed the levels of AVPV *Kiss1* expression at times of LH surge peak and trough in OVX rats with and without E_2 (Fig. 2.2). I found that the *Kiss1* expression values, though no longer significantly different at peak and trough, still show a trend of peak expression and trough expression [n = 4-6; two-way ANOVA for time and E_2 condition yields significant effect of time ($F = 27.8$, $P = 0.008$), of E_2 condition ($P < 0.0001$), and of interaction ($P = 0.038$)]. Post-hoc comparison Tukey Test reveals peak and trough differ with E_2 ($P < 0.05$) but not without E_2. A t-test of peak and trough without E_2 approaches significance ($P = 0.1$). These animals had been released into DD 12-30 hours before sacrifice, suggesting this rhythm is indeed circadian. The trend in animals without E_2 is consistent with a model where E_2 amplifies underlying AVPV activity, but is not conclusive. The question remained as to whether this rhythm is dependent on the SCN.

Because efferents from each SCN almost exclusively reach ipsilateral targets, unilateral lesions of the SCN allowed us to assess the induction of *Kiss1* mRNA expression and the activation of GnRH cells without an SCN, as compared to the intact-SCN side of the same animal. Following electrolytic lesions of the right SCN, the animals were allowed to heal for two weeks. Double

immunohistochemical labeling for GnRH and the cFOS protein in brains taken at the time of the LH surge in OVX-E_2 females revealed that GnRH cells showed significantly more cFOS-positive nuclei on the intact than on the lesioned side of the brain (n = 7 successful lesions, paired t-test, p = 0.004) (Fig. 2.3). This difference disappeared in animals in which the lesion missed the SCN (n = 9 missed lesions, paired t-test, p = 0.08), suggesting that the lack of activation of GnRH cells was due specifically to the loss of the SCN.

Similarly, paired t-tests of optical densities after ISH with a ^{35}S-tagged *Kiss1* riboprobe revealed a significant reduction of AVPV *Kiss1* expression on the lesioned side (n = 5 successful lesions, p = 0.016) (Fig. 2.3). As with GnRH cell activation, this effect disappeared in animals with missed lesions (n = 6, p = 0.33). *Kiss1* expression roughly doubled from its circadian trough to its peak (Fig. 2.1A), as well as from the SCN-lesion side to the contralateral side (Fig. 2.3M). In every animal where GnRH-cFOS colocalization decreased unilaterally, *Kiss1* levels decreased on the same side; similarly in every animal where Kiss1 levels decrease, so did GnRH-cFOS colocalization.

Chapter Discussion.

Taken together, these data indicate that, as with female mice, female rats primed with E_2 show circadian rhythm of *Kiss1* expression in the AVPV, with a peak at the beginning of the locomotor daily activity bout (in phase with the LH surge). These data show a trend which suggest that this AVPV-*Kiss1* expression rhythm may not be E_2-dependent, but rather E_2 modulated, however this needs to be confirmed. Because no other output from the SCN is known to vary so strongly with E_2, this argues that the amplification effect of E_2 is local, within the AVPV.

Whereas the master regulation of circadian locomotor rhythms relies on diffusible factors released by SCN neurons[64], the circadian release of hormones, including melatonin, glucocorticoids and LH, relies on synaptic connections between specific neurons in the SCN and specific extra-SCN neuronal targets[133,136,137]. My data demonstrate that ipsilateral SCN neuronal connections are necessary for the expression of the circadian peak of *Kiss1* in the E_2-primed AVPV, and for activation of GnRH cells in the MPO at the time of the LH surge. Further, they suggest that the activation of GnRH cells during the LH surge is associated with increased *Kiss1* levels, which in turn depend on circadian signals from the SCN. Given the distance that newly synthesized KISS would have to travel to be released onto GnRH cells, it is unlikely that this rise in *Kiss1* expression could lead to changes in KISS levels that could be in fact causing the ongoing surge. More likely is that the SCN input causes both a release of presynaptic KISS, and a concomitant up-regulation in *Kiss1* to replace the KISS pool. The truth of this proposition, and the mechanisms involved, are beyond the scope of this work.

Knowing the sub-region of the SCN responsible for this signal would narrow the potential relevant neurotransmitters informing this *Kiss1* rhythm. VIP-containing fibers, presumably emerging from the vlSCN, project directly to GnRH cells and could be responsible for the induction of cFOS expression within GnRH cells seen here. In contrast, AVP-containing fibers, presumably emerging from the dmSCN, project to the AVPV, and are therefore more likely to affect $KISS^+$ cells. If the *Kiss1* expression rhythm is in fact related to the GnRH surge and LH surge, then the dmSCN alone could potentially be able trigger these events. Alternatively, if the *Kiss1* expression peak is not related to causing the LH surge, then the vlSCN alone might be sufficient to prime GnRH cells and induce an LH surge. Finally, the synchronized activity of both

subregions of the SCN could be critical for the induction of the surge. The next chapter will attempt to address these issues.

Data behind figures 2.1 and 2.3 have been published in Smarr *et al.*, 2012[144].

Figure legends

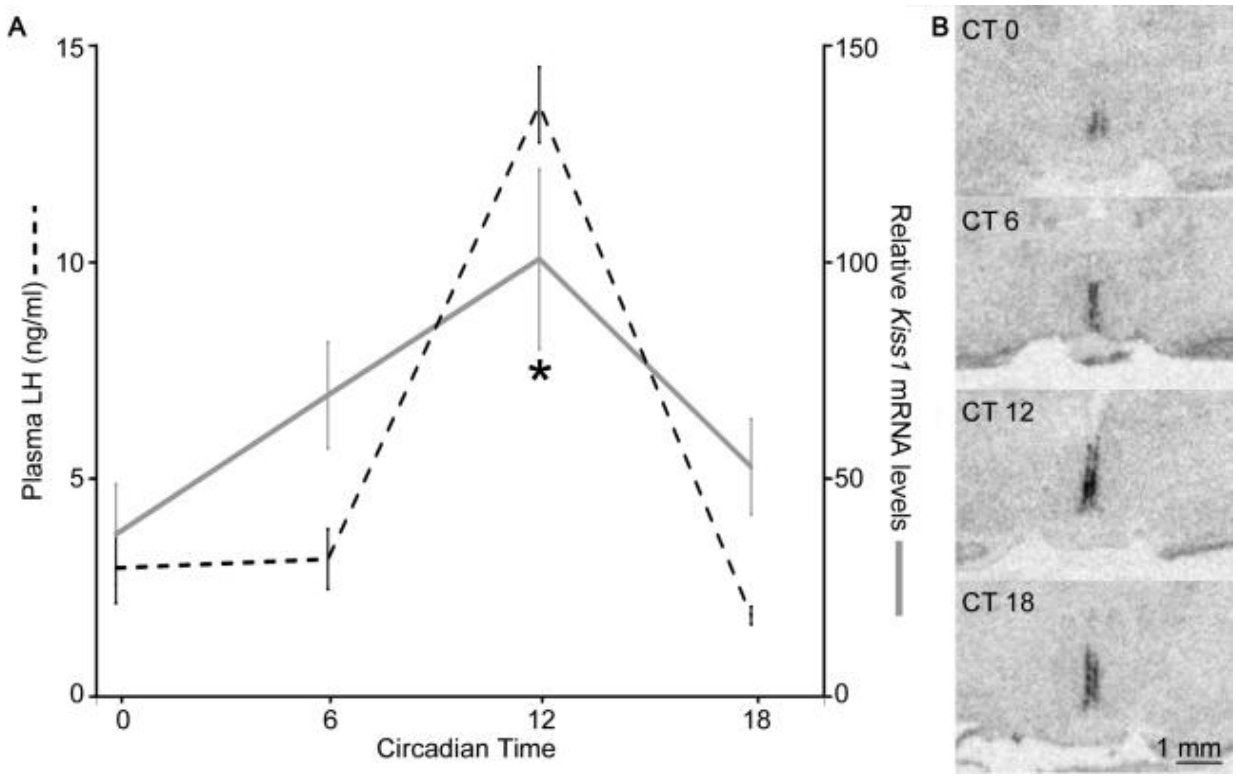

FIG. 2.1. Circadian *Kiss1* expression in the AVPV peaks at the time of the LH surge in OVX+E_2 rats. A, Relative *Kiss1* mRNA levels (grey line) and plasma LH (dashed line). Sample frequency is 1 per 6 h. Data represent mean ± SEM. B, Representative autoradiographic films of coronal sections at the same AVPV level from animals sacrificed at the indicated times and labeled with an antisense *Kiss1* mRNA ^{35}S-tagged riboprobe. One-way ANOVA for *Kiss1* levels, F = 0.023, p = 0.023, n = 4-6 per time point; *, significantly different from CT0, Tukey post hoc comparison, p = 0.05).

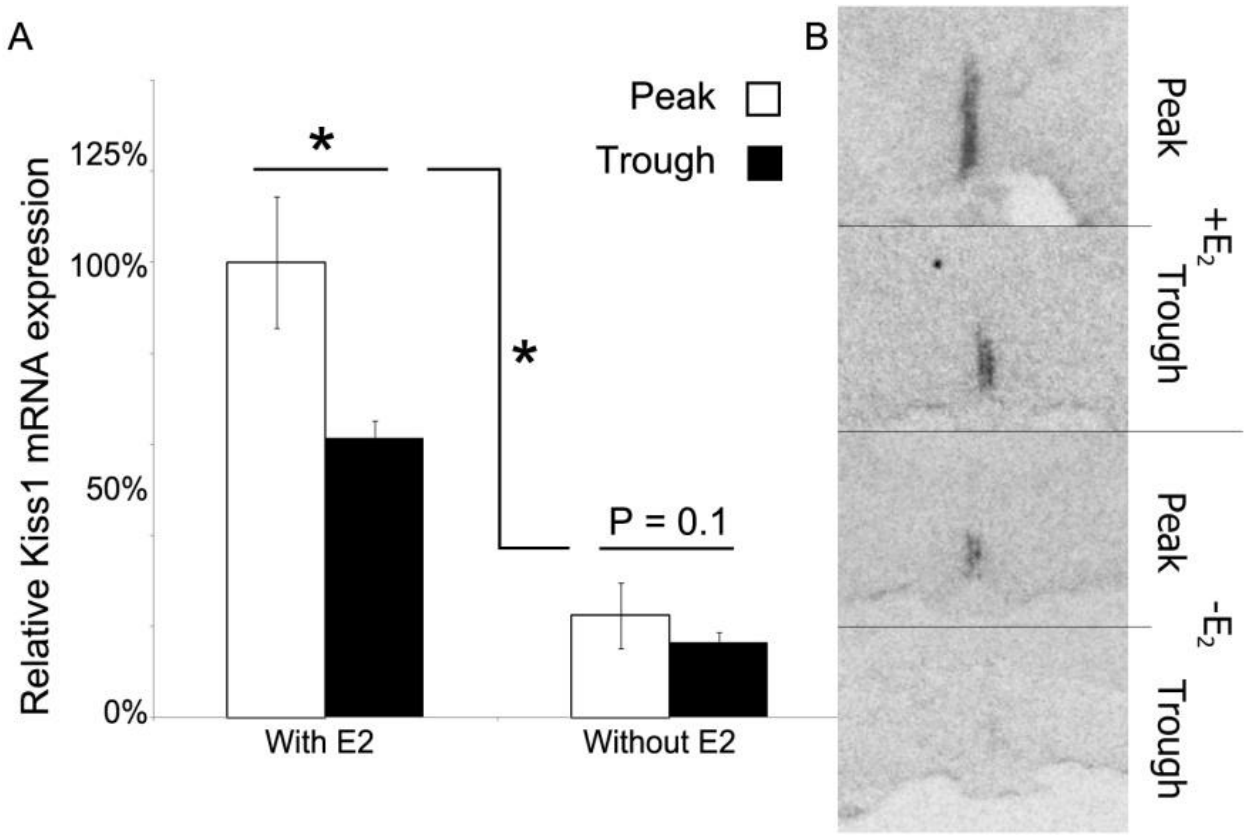

FIG. 2.2. Mean relative values of *Kiss1* expression in the AVPV of OXV rats with or without E_2 implants, taken at the predicted time of *Kiss1* rhythm peak and trough from rats entrained to 12:12 LD, and then released into DD for the day of sacrifice. A two-way ANOVA finds a significant effect of group, time, and interaction (see chapter text); vertical black bar with * indicates significant difference between the "with" and "without" E_2 conditions, as measured by a two-way ANOVA; horizontal black bar with * indicates significant difference between peak and trough times in animals with E_2, as measured by Tukey-Kramer post-hoc analysis ($P<0.05$); Post-hoc analysis of peak vs. trough in the "without E_2" group did not find significance, but a t-test finds the P-value at 0.01, suggesting a trend may persist (A). Representative autoradiographic films of coronal sections at the AVPV level from animals sacrificed at the expected peak and trough times, with or without E_2, for *Kiss1* mRNA expression and labeled with an antisense *Kiss1* mRNA ^{35}S-tagged riboprobe (B).

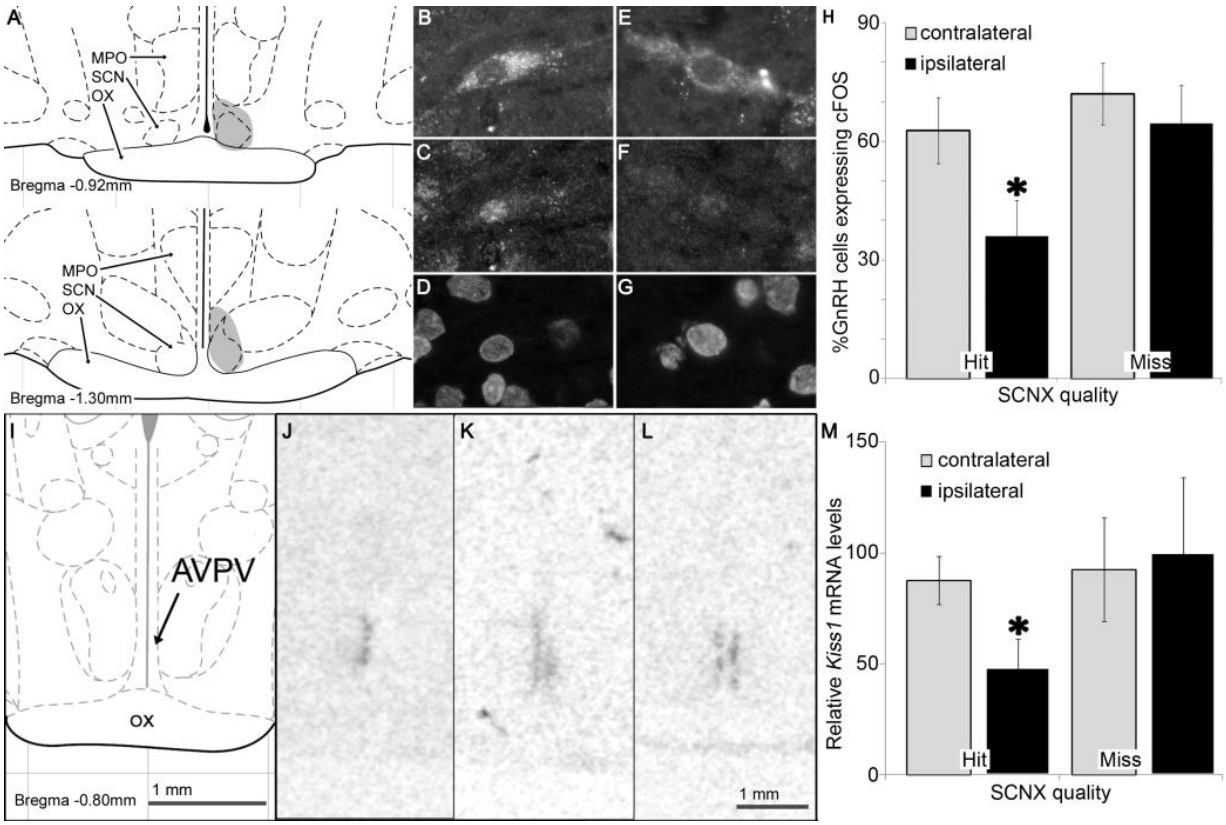

FIG. 2.3. Ipsilateral SCN projections gate the daily activation of GnRH cells and the AVPV *Kiss1* expression rhythms in OVX+E_2 rats. A, Schematic coronal section [modified from (64)] showing the lesion location at two rostrocaudal levels from an animal that received a successful unilateral SCN lesion (shaded). Medial preoptic area (MPO), suprachiasmatic nucleus (SCN), and optic chiasm (OX) are indicated. B-G, Representative confocal photomicrograph of GnRH/cFOS double labeled sections from an animal with a successful lesion. Cells immunostained for GnRH (B, E) cFOS (C, F) and nuclear DAPI stain (D, G) are shown for the contralateral (B-D) or ipsilateral (E-G) side of the lesion. H, The percentage of GnRH cells in the MPO with $cFOS^+$ nuclei is significantly lower on the ipsilateral than on the contralateral side of the lesion in animals with successful unilateral SCN lesions but not in animals in which the unilateral lesion missed the SCN. Bars represent mean ± SEM. *, statistical difference between contralateral and ipsilateral sides within animals (n = 7 successful lesions, paired Student t-test, p = 0.004; n = 9 missed lesions, paired Student t-test, p = 0.08). I, Schematic coronal section at the AVPV level [modified from (64)]. J-L, Representative autoradiographs of coronal sections at the AVPV level from animals sacrificed at the expected peak time for *Kiss1* mRNA expression and labeled with an antisense *Kiss1* mRNA ^{35}S-tagged riboprobe in an animal with a successful unilateral SCN lesion and total loss of ipsilateral *Kiss1* staining (J), a second animal with a successful unilateral SCN lesion and partial loss of ipsilateral *Kiss1* staining (K), and in an animal in which the unilateral lesion missed the SCN (L). M, *Kiss1* expression is significantly lower on the ipsilateral than on the contralateral side of the lesion in animals with successful unilateral SCN lesions but not in animals in which the unilateral lesion missed the SCN. Bars represent mean ± SEM. *, statistical difference between contralateral and ipsilateral sides within animals (n = 5 successful lesions, paired Student t-test, p = 0.016; n = 7 missed lesions, paired Student t-test, p = 0.33).

Chapter 3: Circadian Timing of *Kiss1* Expression and of the LH Surge are Coupled to an Oscillator within the Dorsomedial SCN.

Because the LH surge in females occurs just before locomotor activity onset, we wondered whether either of the two locomotor rhythms emerging under LD22 desynchrony would predict the LH surge in desynchronized females. The outcome of this experiment would point to which oscillator (vl or dm) of the SCN is responsible for timing ovulation. We first confirmed that OVX females display the same behavioral and neural desynchronization as males (Fig.3.1). LD22 led to desynchronization of locomotor activity rhythms in intact females similar to that seen in males, with two statistically significant rhythmic components (22 h and ~25 h) within each individual. ISH with a ^{35}S-tagged *rPer1* riboprobe of OVX females revealed similar anatomical and temporal patterns as previously seen in males[132,145], with the 22-h and ~25-h locomotor activity rhythms associated with clock gene expression within the vl- and dmSCN, respectively. After desynchronization was confirmed, ovariectomy and subsequent estrogen implantation did not noticeably perturb desynchronization.

The stability of the forced desynchrony protocol allows for the prediction of the phase relationship between the two locomotor activity rhythms, and therefore between the rhythmic clock gene activities of the vl- and dmSCN. In days of maximum misalignment, one locomotor activity bout starts as the other ends; in contrast, in days of maximum alignment, both locomotor activity bouts start at the same time. LD24 control animals showed the expected LH surge timing, with levels of LH rising towards the evening and peaking at the time of lights off (Fig. 3.2C). LD22 desynchronized animals displayed a single LH surge, which was always in phase

with the onset of the dmSCN-associated locomotor activity rhythm (Fig. 3.2 A, B). Thus, on aligned days, the LH surge occurred, on average, at the same phase (relative to the LD cycle) as it did in LD24 controls. On misaligned days, however, the LH surge had the same phase relationship to the onset of dmSCN locomotor activity rhythm but no significant relationship to the LD cycle or the entrained vlSCN-associated locomotor activity rhythm. Raleigh tests for clustering of the phases of LH surge onsets for all animals within each group confirmed a significant clustering of onsets for LD24 controls (onset time = lights-off - 2.71 h; n = 7; p = 0.010) and for all desynchronized animals relative to the dmSCN locomotor activity rhythm, whether they had been bled during aligned (onset time = lights-off – 2.49 h; n = 10; p = 0.0018) or misaligned days (onset time = dmSCN-associated locomotor activity onset - 3.35 h; n = 9; p = 0.013). Clustering relative to the vlSCN locomotor activity rhythm was only significant for animals bled during aligned days (onset time = lights-off + 2.07 h, p = 0.007 for aligned; onset time = lights-off + 4.82 h, p = 0.23 for misaligned). One-way ANOVA for phases revealed no differences between LD24 controls (relative to the LD cycle), LD22 aligned animals (relative to the LD cycle) and LD22 misaligned animals (relative to the dmSCN-associated locomotor activity onset) ($F = 3.422$; $p = 0.47$) (Fig. 3.3). Taken together, these results indicate that regardless of alignment between the vl- and dmSCN neuronal oscillators, the LH surge always occurred in phase with the predicted activity of the dmSCN. Although there is an apparent bifurcation of the clusters on misaligned days relative to the dmSCN-associated rhythm, this probably does not reflect a real biological timing phenomenon. Rather, it likely arises from days in which the misalignment between the 22h and the ~25h rhythms is not complete (See Fig. 3.2B).

The LH surge amplitude, but not duration, was significantly lower in LD24 controls than in LD22 desynchronized animals bled either during aligned or misaligned days (Fig. 3.4). A 2-way ANOVA with group and time as factors yielded a significant effect of group ($F = 26.71$, $p < 0.0001$) time ($F = 23.02$; $p < 0.0001$) and the interaction ($F = 2.51$, $p < 0.0001$). Post hoc Tukey contrasts ($p = 0.05$) indicated that each group was significantly different from the others (LD24 < LD22 misaligned < LD22 aligned). Although the timing of the LH surge in LD24 animals was as expected, the amplitude of their LH surge was lower than expected and lower than the LH surge drawn from trunk blood (see Fig. 2.1).

Our analysis indicates that the LH surge is coupled to the clock gene activity of the dmSCN. Our hypothesis that the circadian gating of *Kiss1* expression is associated with the timing of the LH surge predicts that the peak of *Kiss1* expression should occur just before the dmSCN locomotor activity onset in desynchronized rats. We sacrificed LD22 desynchronized OVX+E_2 females during misaligned days just before the dmSCN-associated locomotor activity onset or just before the vlSCN-associated locomotor activity onset, as well as during aligned days just before the coinciding locomotor activity onsets ($n = 4$ for each of the groups). We assessed *Kiss1* mRNA expression in coronal sections of the AVPV by ISH and found a significant effect of phase (Fig. 3.5; one-way ANOVA, $F = 4.25$, $p = 0.05$). Tukey post hoc contrasts ($p = 0.05$) revealed that whereas the levels of *Kiss1* mRNA in misaligned animals before the dmSCN-associated locomotor activity onset did not significantly differ from those of aligned animals, the levels in misaligned animals before the vlSCN-associated locomotor activity onset were significantly lower. A planned comparison between the levels before the vlSCN-associated locomotor activity onset and the other two groups taken together indicated the expression was lower in

misaligned animals sacrificed during the vlSCN-associated locomotor activity onset ($p = 0.02$). These data indicate that, similarly to the timing of the LH surge, *Kiss1* expression is coupled to the clock gene activity of the dmSCN but not to the activity of the light-entrained vlSCN.

Chapter Discussion.

Our results provide evidence for the identity of the specific SCN subregional oscillators and their downstream targets critical for the circadian timing of the LH surge. As discussed briefly in chapter 1, the dm- and vlSCN are heterogeneous not only under our forced desynchrony protocol but also in their pattern of afferent and efferent projections and their expression of specific neurotransmitters[134]. Whereas neurons synthesizing AVP are localized within the dmSCN, neurons synthesizing VIP reside in the vlSCN. Although SCN neurons send axonal projections to the MPO[136,146], they likely emerge from vlSCN VIPergic SCN neurons[147]. Our findings suggest that this SCN monosynaptic pathway to GnRH cells is likely not responsible for the initiation of the LH surge. Rather, circadian signals emerging from the dmSCN and ovarian estrogen signals likely converge on *Kiss1* cells, which in turn signal GnRH cells to induce the surge.

The rat is the only animal model in which the stable desynchronization of the vl- and dmSCN has been achieved. The specific role of these SCN subregions cannot be addressed by classic neuroanatomical lesions because of the difficulty to individually target them and because vlSCN efferent fibers course through the dmSCN[148]. Thus, the forced desynchronized rat represents a unique model in which the output of each subregion can be dissected out. Although our results in the forced desynchronized OVX+E_2 female rat do not demonstrate a causal link between the

dmSCN activity and the LH surge, the association between this region's clock gene activity and the timing of the LH surge point to the dmSCN as the site of a critical circadian oscillator timing the LH surge.

Our data suggest a role for the vlSCN in modulating the amplitude of the LH surge. Given the mismatch between the amplitude values of circadian profiles (from samples every 6 h under constant darkness in animals released from LD24) and serially bled animals under LD24, it is likely that the LH surge amplitude of this latter group was diminished by the handling schedules, stress of bleeding or other factors. Importantly, there was a difference in LH-surge amplitude between LD22 aligned and misaligned animals, with maximum LH levels in aligned animals, as might be expected if misalignment between oscillators causes incomplete activation of GnRH cells, for instance. These two groups were housed in the same chamber, handled identically and bled simultaneously. This indicates clearly that while the dmSCN may be initiating the surge, the vlSCN may be modulating the surge amplitude through as-yet undefined alternate pathways. Recent studies have pointed to extra-SCN circadian oscillators within several sites of the HPG axis [see reviews in [148,149]]. They include neural centers such as GnRH cells themselves, which express circadian 'clock genes'[36,150–153], as well as peripheral organs such as the anterior pituitary[36] and the ovary [150]. The increased LH surge amplitude in desynchronized aligned animals suggests that stimulation of GnRH cells may be taking place when the GnRH network and/or its downstream pathways to initiate an LH surge are in highly sensitized phases. We speculate that whereas the dmSCN may send the critical signal to initiate the LH surge, the vlSCN may regulate the sensitivity to this signal in downstream targets. Recent work by Kriegsfeld and colleagues in the Syrian hamster suggest the vlSCN could directly gate

the response of GnRH cells[151] and/or disinhibit them by decreased RFRP release[152]. Finally, other signals, directly released by the SCN or by neurons regulated in turn by SCN efferents, could potentially represent a link between the SCN activity and the activity of the GnRH neuronal network [see [140] for a recent review].

The role of AVP and VIP peptides as putative SCN signals triggering the LH surge has been addressed by several laboratories. AVP can have strong stimulatory effects on GnRH and LH release [154–156] and induce LH surges in SCN-lesioned animals [75]. These effects of AVP appear to be indirect since AVP receptors are barely detectable in GnRH neurons in female rats[157], and although evidence for AVP innervation of GnRH cells has been found in the diurnal Nile rat, it is not clear that these fibers are of SCN origin[158]. In contrast, AVPergic—but not VIPergic—fibers that are likely of SCN origin project to and synapse on kisspeptin cells in the AVPV, kisspeptin cells in this region express the AVP receptor APVr1a, and the expression of this receptor in the AVPV is increased by estrogen in OVX rats[151,157,159]. These results, together with the association of the timing of *Kiss1* expression and the LH surge with clock-gene activity in the AVP-rich dmSCN that we describe, are consistent with a critical role of SCN AVPergic cells in the gating of the LH surge though the regulation of *Kiss1*-extressing cells.

SCN VIPergic efferent fibers, on the other hand, project directly to GnRH cells[146]. The functional relevance of these projections is suggested by the fact that GnRH cells express the VIP receptor VIP2[160] and that VIP-innervated GnRH cells show increased *cFos* expression at the time of the LH surge[141]. The specific role of VIP in the regulation of the LH surge is unclear; VIP can either stimulate[161,162] or inhibit[163–166] the release of GnRH and LH depending on the conditions. This

discrepancy could in part be due to the fact that the response of GnRH cells to the peptide depends both on estrogen levels and the time of the day[140]. Our data show that the timing of the LH surge is not guided by the VIP-rich vlSCN, but rather that this region may be setting the phase of extra-SCN oscillators that decode a timing signal emerging from the dmSCN. Application of the major output of the dmSCN, AVP, only seems to cause an LH surge at when applied in the late afternoon. Taken together, these data suggest that AVP release by the dmSCN represents a critical signal to trigger the LH surge but that the circadian sensitivity of its downstream targets may be equally important. Uncovering a putative rhythm in circadian sensitivity of the AVPV is the topic of the next chapter.

Data behind figures 3.1 through 3.5 have been published in Smarr *et al.*, 2012[144].

Figure Legends.

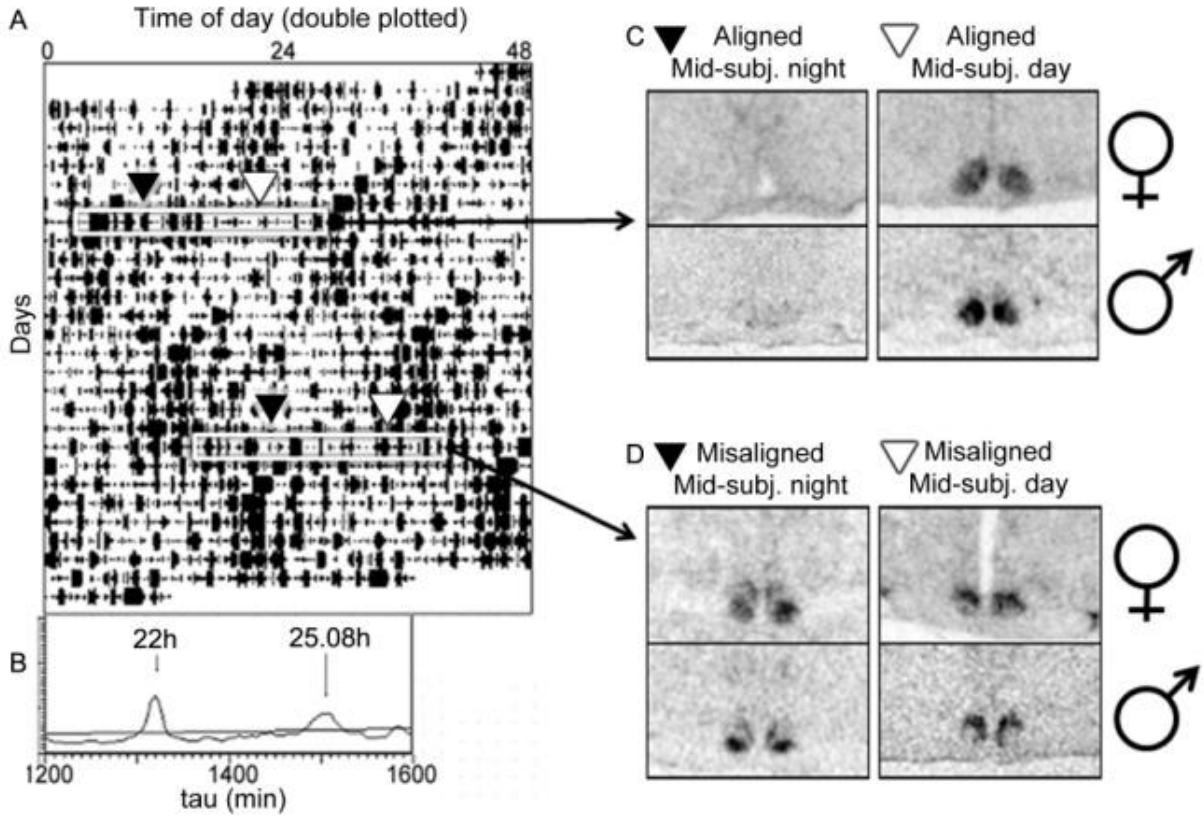

FIG. 3.1. Forced desynchronization of locomotor activity rhythms in OVX+E_2 rats is associated with rhythmic clock gene expression in the vl- and dmSCN. A, Representative actogram of an LD22 desynchronized female; arrowheads represent the specific phases at which other individual animals were sacrificed to process their brain for *Per1* in situ hybridization, n = 2 per time-point. B, X^2 periodogram analysis detects 2 statistically significant rhythmic components of 22 h and 25.08 h in the representative animal shown. C, D, Autoradiographic films of SCN *Per1* expression in animals sacrificed on the phases indicated by the triangles in (A) in a typical desynchronized animal (note that the animal whose actogram is shown was not sacrificed for this experiment). Females sacrificed on aligned days (C) show low levels of *Per1* mRNA throughout the SCN during the dark phase and high levels during the light phase. During misaligned days the pattern of expression between the two subregions is 180º out of phase: the dmSCN shows daytime levels of *Per1* expression during the subjective day (rest) of the ~25-h locomotor activity rhythm whereas the vlSCN shows daytime levels of *Per1* expression during the light phase of the 22-h day (subjective night for the ~25-h locomotor activity rhythm). For comparison, the *Per1* expression pattern in LD22 desynchronized males is shown [modified from (26)] to convey the similarity between the male and female neural bases of circadian desynchrony).

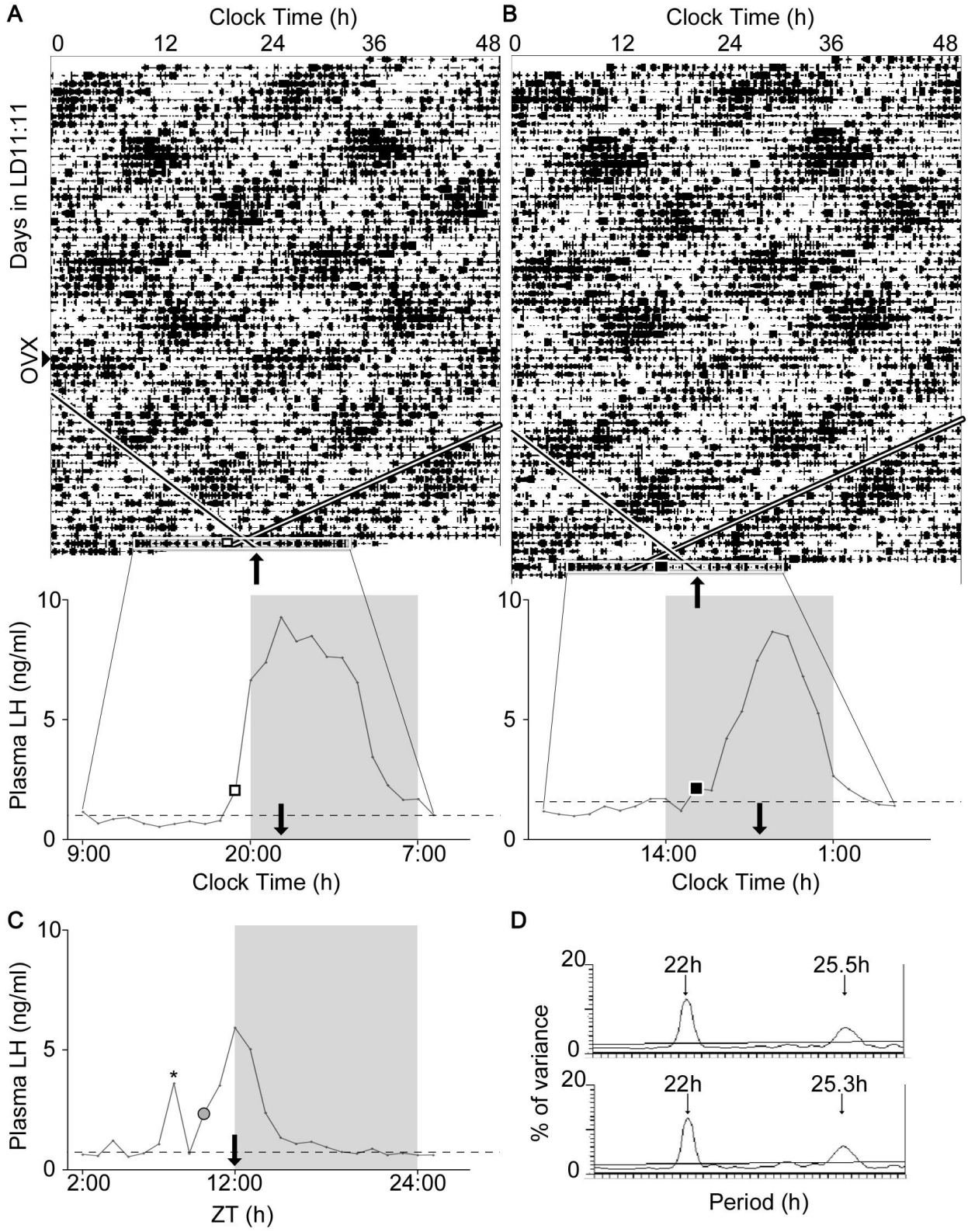
A
Clock Time (h)
0
12
24
36
48
Days in LD11:11
OVX
B
Clock Time (h)
0
12
24
36
48
Plasma LH (ng/ml)
10
5
0
9:00
20:00
7:00
Clock Time (h)
10
5
0
14:00
1:00
Clock Time (h)
C
Plasma LH (ng/ml)
10
5
0
*
2:00
12:00
24:00
ZT (h)
D
% of variance
20
0
22h
25.5h
20
0
22h
25.3h
Period (h)

FIG. 3.2. The circadian timing of the LH surge is coupled to an oscillator within the dorsomedial SCN. A, B, Double plotted actograms (top) and hourly LH profiles (bottom) of two representative LD22 desynchronized OVX+E_2 rats bled during either an aligned day (A) or a misaligned day (B). Arrowhead on left indicates day of ovariectomy for both animals. On actograms, black bars represent locomotor activity, single diagonal lines indicate onset of dmSCN-associated locomotor activity bout with the angle set to match the LD-dissociated period indicated in the periodogram (D), double diagonal bands indicate the time of lights-off. Note that in A the two trend lines cross between the day of bleeding and the preceding day, with the LD-dissociated locomotor activity onset roughly overlapping with the time of lights-off, while in B the LD-dissociated locomotor activity onset beings approximately 7 h after lights-off. The day of bleeding is highlighted as in figure 3.1. Thin black lines expand the 24-h time scale on the bleeding day to easily visualize the plasma LH profiles shown below. Squares indicate the time of the LH surge onset both in the actogram and on the LH profile. Up-facing black arrows indicate the onset of the LD-dissociated locomotor activity in both actograms, and down-facing black arrows indicate the same locomotor activity onset on the LH plots. X-axes are in clock time, to match the actograms. C, Plasma LH profiles in a representative LD24 animal. The gray circle represents the LH surge onset; black arrow indicates the onset of locomotor activity, as in A and B. C, X-axis is in Zeitgeber time (ZT) with ZT12 = time of lights-off. *, a high-LH point not considered part of the surge due lack of contiguity (see methods). D, Periodograms of animals shown in A (top) and B (bottom).

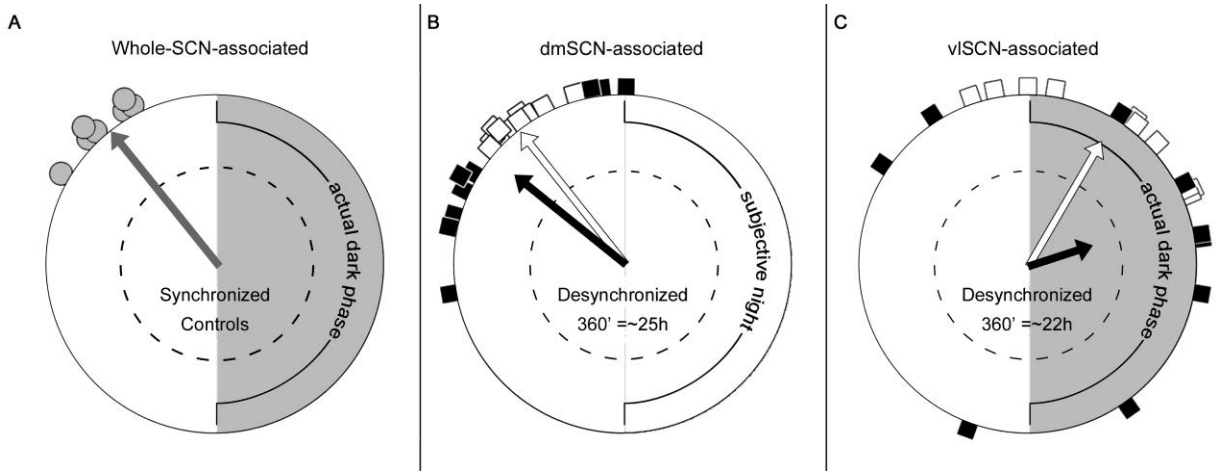

FIG. 3.3. The circadian timing of the LH surge is coupled to an oscillator within the dorsomedial SCN. A, Polar plot and Rayleigh test shows significant clustering of LH surge onset in OVX+E_2 control animals (gray circles, as in Fig. 3.2.C.) with a mean of 2.71 h before lights-off and locomotor activity onset. Vector direction indicates mean phase with 360 º = 24 h, and vector length indicates significance (so a vector extending past the dotted line implies a statistically significant cluster) (n = 7, Rayleigh test, p = 0.010; dotted circle indicates a p = 0.05). B, C, Same as for (A) but for LD22 OVX+E_2 animals. Animals bled during misaligned (points as black squares, descriptive vector in black) and aligned days (points as white squares, descriptive vector in white) are represented in polar plots in which each individual animal's LH-surge onset is plotted relative to the period of one of its locomotor activity rhythms set equal to 360º. Thus, 360º corresponds to the period of the dmSCN-associated activity bout (~25 h) (B) or to the period of the vlSCN-associated activity bout (22 h) (C). Note that the LH surges of animals bled during misaligned days do not significantly cluster relative to the period of the vlSCN-associated activity rhythm (black arrow in C does not reach significance). LD22 Rayleigh tests: B, Days of alignment: n = 10, p = 0.0018, mean phase 2.49 h before locomotor activity onset; days of misalignment: n = 9, p = 0.013, mean phase 3.35 h before locomotor activity onset; C, Days of alignment: n = 10, p = 0.007, mean phase 2.07 h after lights-off and locomotor activity onset; days of misalignment: n = 9, p = 0.23.

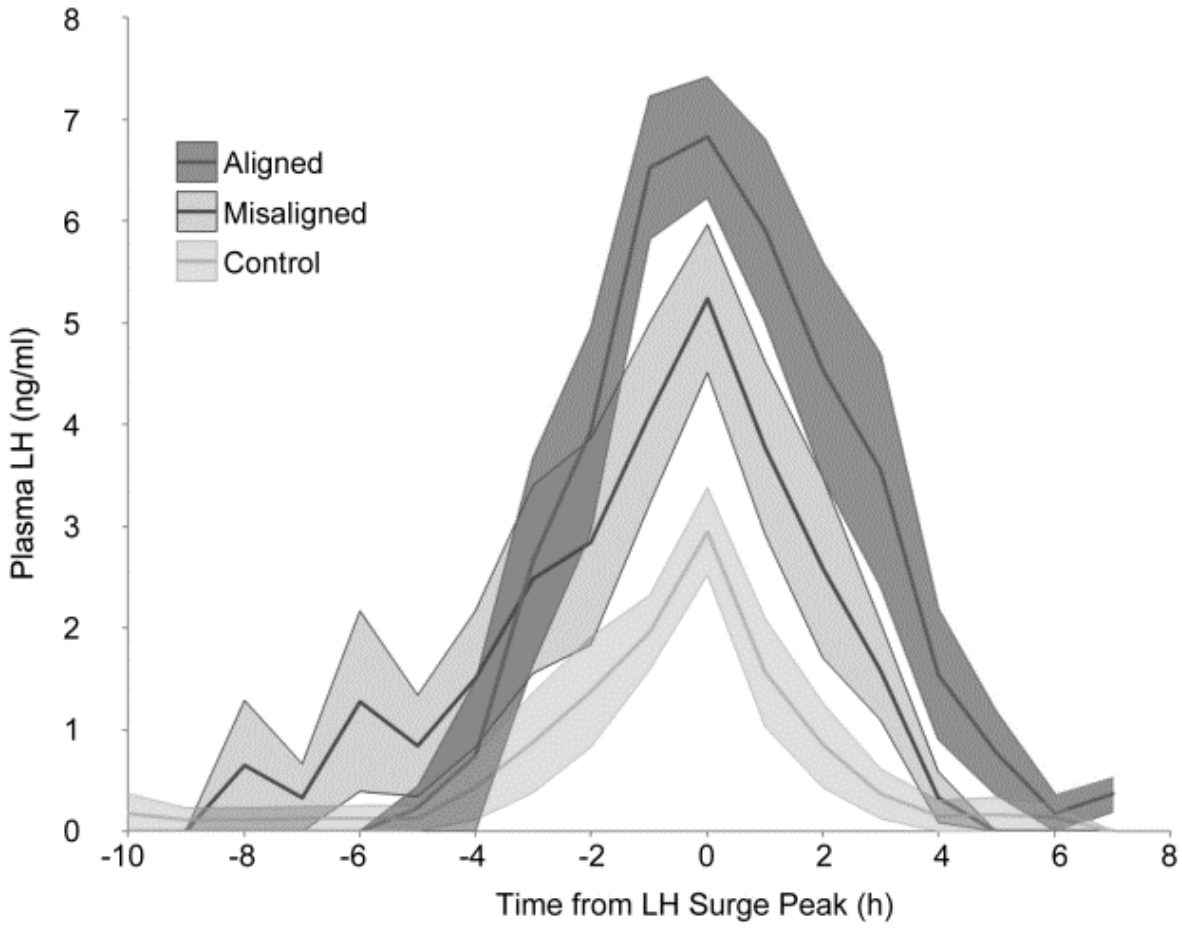

FIG. 3.4. Circadian desynchronization affects the LH surge amplitude. Means ± SEM of LH surges centered at their peak time (0), grouped by phase on the day of bleeding. Each group is significantly different from each other (2-way ANOVA, effect of group, $F = 26.71$, $p < 0.0001$; time, $F = 23.02$; $p < 0.0001$; and the interaction, $F = 2.51$, $p < 0.0001$).

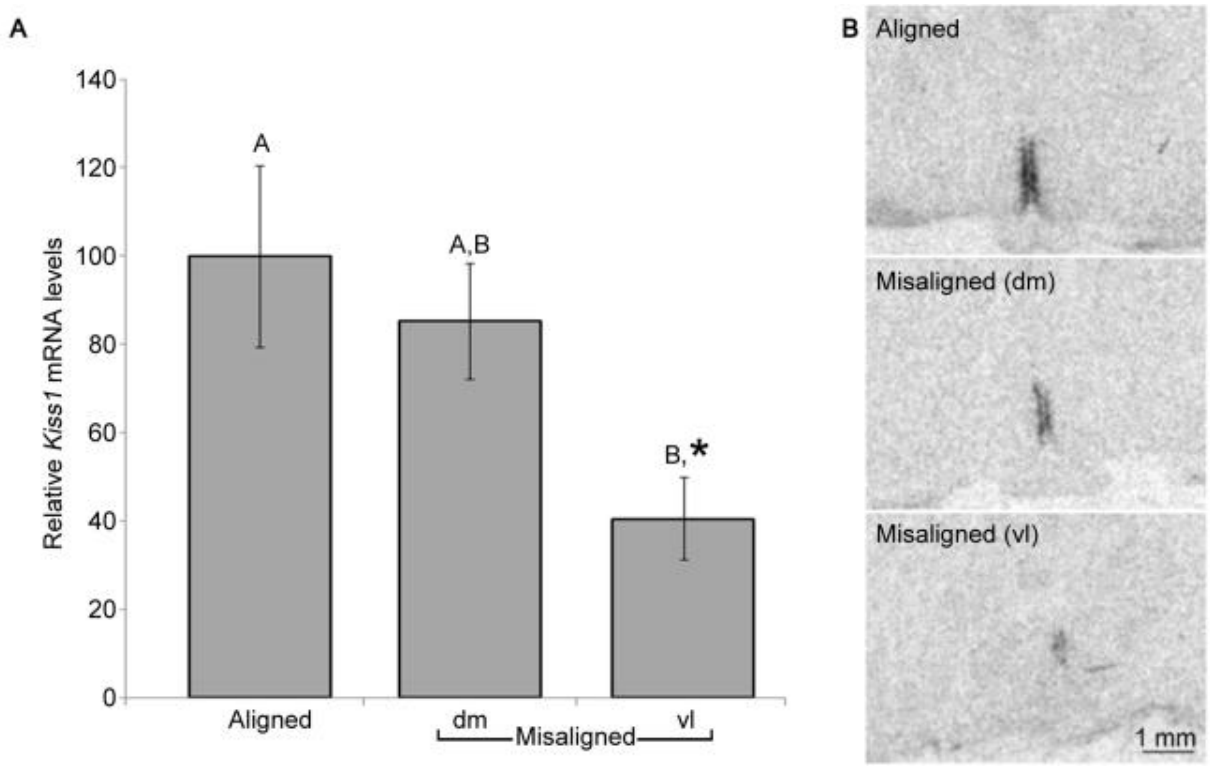

FIG. 3.5. Circadian *Kiss1* expression is coupled to an oscillator within the dorsomedial SCN. A, *Kiss1* expression on misaligned days 1 h before dmSCN-associated activity onset ,but not 1 h before the vlSCN-associated locomotor activity onset, is similar to that in aligned animals before the locomotor activity onset. One-way ANOVA ($p = 0.05$). Bars represent mean ± SEM; groups not sharing the same capital letter are statistically significantly different according to Tukey post hoc comparisons ($p = 0.05$). *, significantly different from aligned and misaligned taken together, planned comparison, $p = 0.02$. B, Representative *Kiss1* in situ hybridization autoradiographic films from animals sacrificed on aligned days just before locomotor activity onset, and on misaligned days just before dmSCN-associated activity onset (dm) or just before the vlSCN-associated activity onset (vl).

Chapter 4: Distal vs. Proximal Regulation of AVPV Kiss1 Expression.

So far my data do not explain the nature of the connection between the dmSCN and the AVPV. As stated previously, the dmSCN releases AVP as a principal neurotransmitter, and the AVPV expresses the AVPr1a receptor, the expression of which is increased by E_2 in OVX female rats[151,157,158]. AVP has also been shown to rescue a surge in SCN lesioned, OVX+E_2 female rats[75]. In SCN intact rats, AVP has a significant impact on the surge amplitude, but only when applied in the late afternoon – the time before the LH surge would normally be triggered anyway[154]. In other words, AVP's efficacy is phase dependent, suggesting that the sensitivity to the SCN neuropeptide in its AVPV targets is modulated in a circadian fashion. This modulation of sensitivity could be achieved by the SCN itself or, alternatively, could be locally controlled by an extra-SCN oscillator located within the AVPV itself. To test this latter possibility I assessed the expression of the clock gene *Per1* within the AVPV. Using alternate sections from the brains used to measure circadian *Kiss1* expression rhythm in Chapter 2, I assayed *Per1* levels at the same AVPV levels that showed *Kiss1* expression. I found a significant rhythm in AVPV *Per1* expression with a peak around the time of the LH surge [n = 4-5 per time point, one-way ANOVA for time found a significant effect ($F = 11.73$, $P = 0.0003$)]. A post-hoc Tukey-Cramer comparison between peak and trough found a significant difference ($P < 0.05$) (Fig. 4.1).

If the AVPV contains an extra-SCN oscillator, then the results from chapter 3 suggest this oscillator is entrained by the dmSCN. One prediction of this hypothesis is that the *Per1* rhythm should remain in phase with the dmSCN under internal desynchronization. To test this, I assessed *Per1* expression in the AVPV of desynchronized rats. I found no detectable difference in *Per1* expression intensity between the onset of dmSCN-associated locomotor activity on days

of alignment and misalignment. In contrast, on days of misalignment, *Per1* levels at the time of the vlSCN-associated locomotor activity onset were significantly lower than at the time of the dmSCN-associated locomotor activity onset [n = 4 per time point, one-way ANOVA for phase found a significant effect ($F = 8.98$, $P = 0.007$). Post-hoc Tukey comparison found a difference between the AVPV *Per1* expression before the vlSCN-associated activity onset on misaligned days and the expression before activity onset before the the dmSCN-associated activity onset on aligned or misaligned days ($P < 0.05$) (Fig. 4.2). By contrast, there was no detectable difference between the expression before the activity onset in aligned days and before the dmSCN-associated locomotor activity in misaligned days ($P > 0.05$). These data support the hypothesis that the AVPV contains an extra-SCN circadian oscillator entrained by the dmSCN.

My data in forced desynchronized rats suggested that a population of oscillators within the AVPV is modulating sensitivity to dmSCN signals in a circadian fashion. This is also consistent with the phase-specific ability of AVP to induce LH release in SCN-intact females. Furthermore, the AVP receptor AVPr1a is expressed within the AVPV in an estrogen-dependent manner, and is expressed within AVPV $KISS^+$ cells. These findings suggest the AVPr1a receptor is at a nodal point to sense circadian signals from the dmSCN. If the AVPV undergoes phasic changes in sensitivity to the AVPergic dmSCN, I hypothesized that AVPr1a is a clock output of the circadian oscillators within the AVPV. To test this possibility I assayed the levels of *AVPr1a* mRNA by ISH in the AVPV of E_2-primed rats at different circadian phases. I found that in E_2-primed animals, there was a significant rhythm of *AVPr1a* expression in the AVPV [n = 3-5 per time point, significant effect of time, one-way ANOVA ($F = 5.5$, $P = 0.013$)]. A post-hoc Tukey comparison between peak and trough found a significant difference ($P < 0.05$) (Fig. 4.1).

Chapter Discussion.

Taken together, the data in this chapter support the idea that the AVPV contains an extra-SCN oscillator entrained to the dmSCN, as opposed to a simple output relay for signals from dmSCN. It further suggests that this oscillator could act as a clock, regulating *Kiss1* and *AVPr1a* expression. Together, my results support a model in which the AVPV serves as an integration hub for the ovulatory cycle through E_2 and the circadian cycle through AVP from the dmSCN. According to this model, high E_2 during proestrus unmasks a phase coincidence between the dmSCN circadian AVP signal and its sensitivity within the AVPV.

It is interesting to note that the *rPer1* rhythm we find here in the AVPV is 90°out of phase with the rhythm in the SCN. While it is a novel finding in the AVPV, other peripheral oscillators, including the pituitary, are also out of phase with the SCN[58]. This suggests that while clock gene oscillations must be coherent in period within the body, phase of each clock gene's rhythm is not globally important.

It is also interesting to note that the shape of the region with the AVPV stained positive for *Kiss1* – roughly vertical lines on either side of the third ventricle – appears to differ from the region stained positive for *Per1* and *AVPr1a*, both of which stain a region more triangular and extending slightly more ventral. This difference suggests that the circadian oscillating population of cells within the AVPV may be different, or only partially overlap with the population of Kiss cells in the AVPV. Ideally, triple labeling for AVPr1a, Per1, and Kiss would clarify the extent of overlap of the cellular populations responsible for the staining seen here. The result of such colocalization studies will help elucidate the way in which the AVPV

integrates circadian information into Kiss output, but these studies are beyond the scope this dissertation.

Regarding the AVPr1a data, it is worth noting that the SP6 enzyme used to generate the *AVPr1a* probe may have had reduced activity, and has typically less activity than the T3 and T7 enzymes used for the *Kiss1* and *rPer1* probes, resulting in a weaker ^{35}S probe for *AVPr1a* and a lower signal/noise ratio. A stronger probe might reveal greater differences than those reported here. Also, the time-step of 6h, while mathematically sufficient to describe a rhythm, does not have sufficient resolution to precisely define a peak. If the role of the increase in *AVPr1a* receptor expression is indeed to enhance sensitivity to AVP released by the SCN, peak expression ought to precede the LH surge by at least 1-2 hours (possibly more) to allow for translation and translocation to the membrane, depending on the specific dynamics of Kiss1 activation and transcription/translation. These data do not have sufficient resolution to address this issue. Alternately, the increase in AVPr1a mRNA could be to regenerate the pool of receptor protein if it becomes deactivated and degraded following AVP binding. Further investigation in to the precise timing of AVPr1a mRNA and protein cycles would help resolve this ambiguity.

Finally, functional assays in brain slices through the AVPV of female rats showing differential $KISS^+$ cell responsiveness to AVP at different circadian times and/or under different E_2 treatments would resolve the mechanistic regulation of the model presented here, but lack of $KISS^+$ cell markers renders this technically unfeasible as of the time of this writing.

Figure Legends

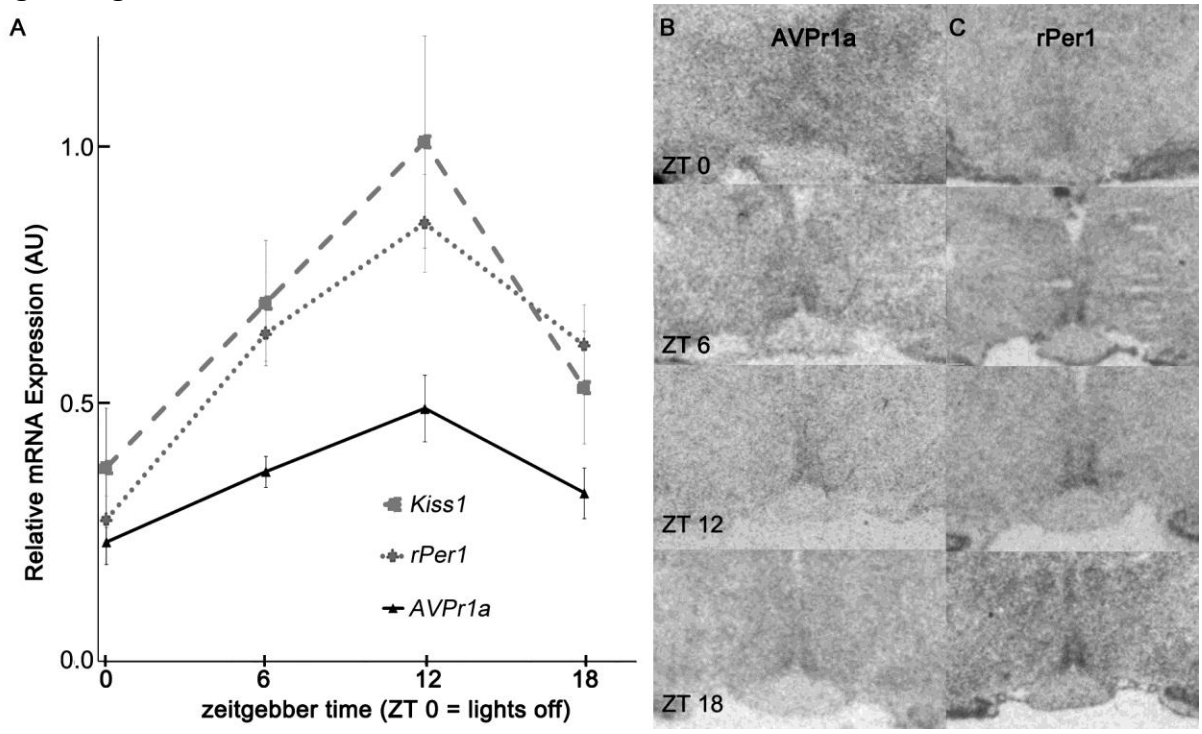

Figure 4.1. Circadian rhythms in *Kiss1*, *rPer1*, and *AVPr1a* in the AVPV of OVX+E2 rats, as measured by ^{35}S-probe ISH on alternating sections of the same AVPVs with each probe. ANOVA of each curve shows significant effect of time, and post-hoc analysis of each curve by Tukey-Cramer finds that each curve's peak significantly differs from its trough value. *Kiss1* curve is recreated from Fig. 2.1. (A). Representative radio-photomicrographs at each time point for AVPr1a (B) and rPer1 (C).

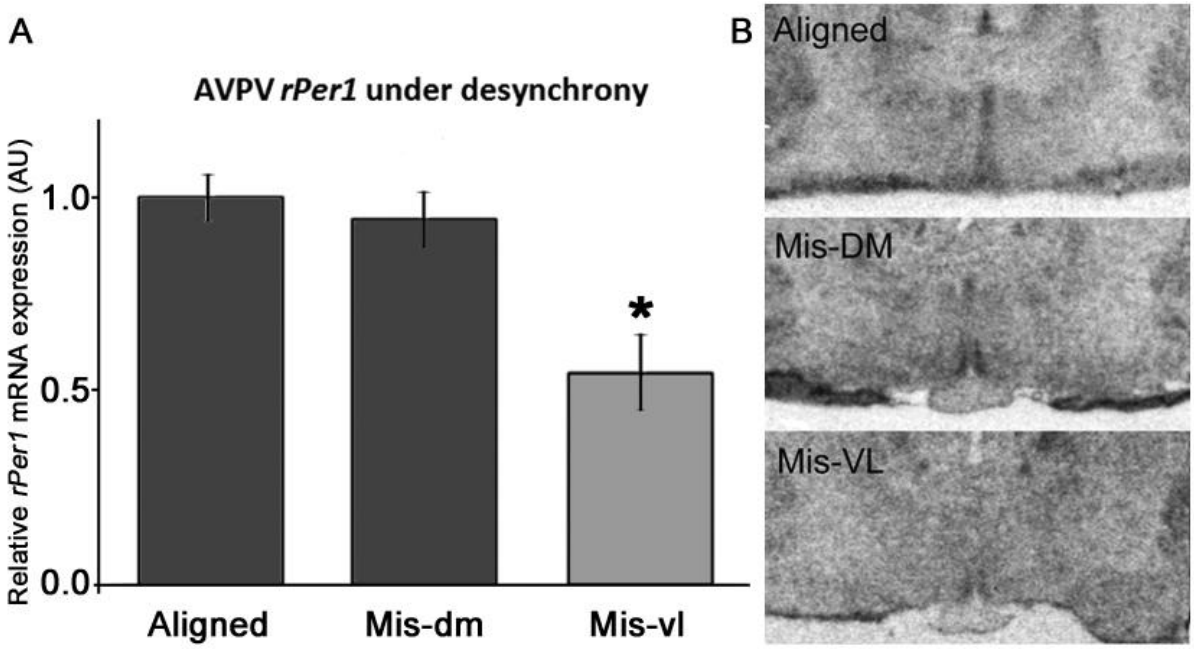

Figure 4.2. Mean *rPer1* expression in the AVPV of internally desynchronized OVX+E2 rats, as measured by ^{35}S-probe ISH. ANOVA shows significant effect of phase, and post-hoc Tukey analysis finds that rPer1 expression is significantly diminished before onset of the vlSCN-associated locomotor activity bout in misaligned days (Mis-vl), but not before onset of dmSCN-associated locomotor activity bout (Mis-dm), as compared to AVPVs measured before the onset of locomotor activity on days of alignment (Aligned) (A). Representative radio-photomicrographs of labeled AVPVs from each phase (B).

Chapter 5. Final Discussion.

Circadian biology and female reproductive endocrinology were first formally joined by Everett and Sawyer in 1950[167], when the pair demonstrated that ovulation could be pharmacologically blocked during a short window of time on the afternoon of proestrus. Ovulation did not occur upon removal of the blockade, but rather 24 hours after it should have occurred. This demonstrated that the LH surge depended not just on hormonal priming, but specifically on timing. In 1980 Coen *et al.*, showed that lesions of the SCN resulted in loss of the LH surge[74]. When it became clear in 1990 that the SCN was the mammalian master circadian pacemaker[53], these and other pieces of evidence suggested strongly that SCN afferents were the source of the timing signal needed for the LH surge. Although connections from the SCN to GnRH cells have been shown, tests on GnRH cells of major SCN outputs like GABA, AVP, and VIP have not been convincing as triggers for the LH surge (see chapter 3 discussion for details on this). Meanwhile, in the 2000s Kiss1 was found to be the strongest known driver of the GnRH cells, and able to stimulate an LH surge (see "Kisspeptin and its Regulation of GnRH release" in the chapter 1 for details on Kiss1). This dissertation provides evidence for a new map connecting the SCN to GnRH cells specifically to time the onset of the LH surge. The proposed map links the dorsomedial SCN to an oscillating population of neurons within the AVPV by way of AVP. This AVPV population coordinates *Kiss1* expression rhythms in the AVPV when E_2 is present at sufficient levels to suggest the pre-surge time of the reproductive cycle. This *Kiss1* rhythm in turn is linked to Kiss1 release rhythms onto GnRH cells. In addition, this dissertation provides information in support of an answer to the question of how ovulatory timing is regulated: that there is not a single circadian signal, but many circadian components, both

signals and receivers, all of which must be aligned for optimal reproductive health and a "normal" LH surge.

There has been considerable debate about how the SCN gates the LH surge. My data provide strong support for the hypothesis that GnRH cells in the MPO are timed by multi-synaptic rather than monosynaptic input from the SCN. My data also support a role for AVPV kisspeptin cells as an SCN relay station that confers circadian timing information to GnRH cells, and as a likely site for the integration of time-of-day and time-of-cycle information necessary for the surge to occur. I show that AVPV *Kiss1* circadian expression and GnRH neuronal activation are both dependent on ipsilateral input from the SCN. Furthermore, I show that both the expression of *Kiss1* in AVPV neurons and the LH surge are phase-locked to a circadian oscillator located within the dmSCN, but not to the oscillations within the vlSCN. Finally, I show that the AVPV could itself be a circadian oscillator, with circadian rhythms of the clock gene *Per1* in the AVPV ~90°out of phase, but entrained to, the dmSCN, and a circadian clock output of *AVPr1a*.

My data allow me to suggest the following model for how these two oscillators – the HPG-driven ovulatory rhythm and the SCN-guided circadian rhythm – integrate their information to time the neural decision to trigger ovulation (Fig 5.1.). In this model the AVPV monitors both ovarian E_2 levels to mark ovulatory phase, and dmSCN AVP to mark circadian phase. E_2 reception within the AVPV unmasks the circadian expression of AVPr1a, allowing phase-specific, E_2-dependent sensitivity to daily dmSCN AVP output only on the day of proestrus. Thus at the right time of day – late afternoon in the rat – on the day of proestrus

only, the AVPV becomes hyper-receptive to a signal from the dmSCN to release, and then replace, a pool of Kisspeptin onto GnRH cells of the MPO.

This model predicts that ovulation and the LH surge timing and shape should be disrupted if the SCN is desynchronized or the SCN and AVPV misaligned. In animal models, internal desynchrony and misalignment of peripheral oscillators from the SCN are both hallmarks of circadian disruptions similar those in humans under rotating shift work or repeated exposure to jet lag in humans. Nearly 20 million Americans work on nocturnal shifts (Department of Labor, 2007), as presumably do many more people worldwide. Women working under this disruptive temporal environment are significantly more likely to suffer severe reproductive ailments including irregular menstrual cycles, reduced fertility, miscarriages, and preterm births[78–80]. Although the causes for these increased health risks are unknown, a salient feature in humans under nocturnal shift-work is the internal desynchronization of circadian rhythms[168,169]. Progress in understanding the adverse health consequences of circadian internal desynchronization has been slow because of the lack of animal models in which desynchronization can be stably induced. Rats are the only rodent in which the vl- and dmSCN can be stably desynchronized and the result of this desynchronization on the regulation of circadian outputs bears remarkable similarities with the regulation of outputs in humans under forced-desynchrony protocols[170,171]. Thus, the forced desynchronized rat offers a unique opportunity to not only dissect out the independent circadian outputs of the vl- and dmSCN but also to study the mechanisms underlying adverse physiological consequences of circadian internal desynchrony in a genetically, neurologically and pharmacologically intact animal. My results clearly show that circadian internal desynchronization leads to a timing of the LH surge that is at odds with the LD

cycle and the behavioral and physiological rhythms that are associated with it. Reproductive ailments in women exposed to temporal challenges such as nocturnal shift-work may emerge from a similar misalignment between an LH surge timed by a clock that fails to synchronize to the nocturnal shift and physiological processes that adapt to this abnormal temporal environment.

Both the circadian system and the female reproductive system have immense impacts on an organism's selection of behavior. Yet both, by virtue of being periodic, show predictable change in their outputs. This combination of predictability, tractability and overt behavioral modulation is very rare in neurobiology. As such these systems provide valuable tools in uncovering the sites of information integration used by neural systems to render behavioral decisions; in this case we are able to predict the timing of the "decision" to initiate the LH surge under normal or perturbed conditions. Both the circadian system and the HPG axis modulate affect, arousal, and response to social cues, Although understanding these behavioral outputs has high intellectual and societal value, they are hard to predict or too subtle to easily measure in animal models. The predictable impacts of the HPG axis and the circadian system on behavioral choice offer a unique entrée into difficult-to-approach behavioral neuroscience questions, such as how a female rat switches from aggressive to sexually receptive when presented with a potential mate at the right time.

The term decision does not often apply to hypothalamic output. Usually decision is reserved for neural output applying to targeted, precise, conscious behavior, such as "deciding" to turn left versus right at an intersection. "Consciousness" is yet to be defined by the

neuroscience community. Until it can be precisely defined as a sub-category of neural processes, focusing only on cortical or limbic neural outputs as “decisions” seems like an unfounded limitation self-imposed by the field of behavioral neuroscience. Thus, I use the term “decision” in this work specifically to highlight the false – or at least as yet unjustified – dichotomy between neural-integrator outputs viewed as conscious and unconscious. The inclusion of “unconscious” decision-making circuits, like those described here, would contribute greatly to the tools available for the study of neural integration and behavioral guidance, which is hard enough as it is and does not need artificial restrictions imposed on it.

Figure Legends.

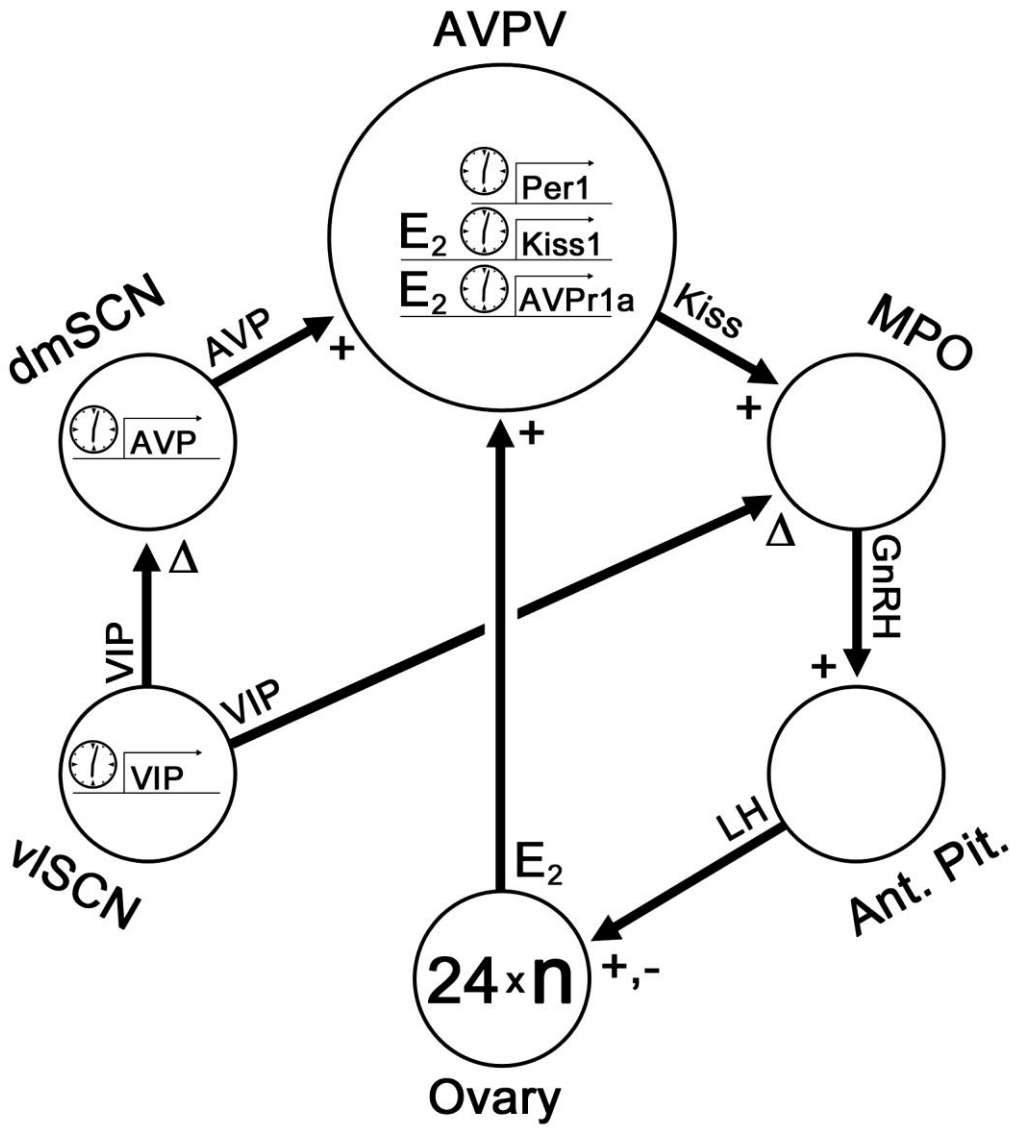

Figure 5.1. Model of integrating circuitry for generating the decision to ovulate. The vlSCN oscillates with a circadian period entrained to the environmental LD cycle. Using VIP and other signals the vlSCN entrains the circadian oscillator within the dmSCN. The dmSCN produces and releases AVP into the AVPV in a circadian fashion. The AVPV also has circadian oscillations, but circadian expression of *AVPr1a* and *Kiss1* are unmasked only when E_2 is present at sufficient concentrations. Under such conditions, the AVPV becomes receptive to SCN AVP, signaling GnRH cells in the MPO with Kiss release while increasing *kiss1* expression to replace the used Kiss. The GnRH cells in the MPO then signal the anterior pituitary (Ant. Pit) with GnRH to release LH into the systemic blood stream. The response by the MPO to Kiss is modulated but not triggered by the vlSCN, possibly using VIP. The ovary, receiving the LH signal, initially increases E_2, but then following follicular rupture decreases E_2 production for a species-specific number of days (n), preventing the LH surge from happening again for n days.

Note: This model focuses only on those oscillators and transmitters discussed within this dissertation. The SCN produces more than just VIP and AVP, there is evidence for circadian oscillators within the MPO, the pituitary, and the ovaries, and there is more information than E_2 concentration and time of day involved in control of triggering the LH surge. This model is not meant to explain all aspects of LH surge modulation, but to provide a testable framework which accounts for the data presented in this work.

References

1. Schiavi R, Jutisz M, Sakiz E, Guillemin R. Stimulation of Ovulation by Purified LH-Releasing Factor (LRF) in Animals Rendered Anovulatory by Hypothalamic Lesion. *Proc Soc Exp Biol Med*. 1963;114:426–429.

2. Caligaris L, Astrada JJ, Taleisnik S. Release of luteinizing hormone induced by estrogen injection into ovariectomized rats. *Endocrinology*. 1971;88:810–815.

3. Guillemin R. Physiology and chemistry of the hypothalamic releasing factors for gonadotropins: A new approach to fertility control. *Contraception*. 1972;5(1):1–19.

4. Brown-Grant K, Raisman G. Abnormalities in reproductive function associated with the destruction of the suprachiasmatic nucleus in female rats. *Proc.R.Soc.Lond.[Biol]*. 1977;198:279–296.

5. Wiegand SJ, Terasawa E, Bridson WE, Goy RW. Effects of discrete lesions of preoptic and suprachiasmatic structures in the female rat. *Neuroendocrinology*. 1980;31:147–157.

6. Ronnekleiv OK, Kelly MJ. Plasma prolactin and luteinizing hormone profiles during the estrous cycle of the female rat: effects of surgically induced persistent estrus. *Neuroendocrinology*. 1988;47:133–141.

7. Kelly MJ, Garrett J, Bosch MA, et al. Effects of ovariectomy on GnRH mRNA, proGnRH and GnRH levels in the preoptic hypothalamus of the female rat. *Neuroendocrinology*. 1989;49(1):88–97.

8. Dierschke DJ, Bhattacharya AN, Knobil E. Circhoral oscillations of plasma LH levels in the ovariectomized rhesus monkey. *Endocrinology*. 1970;87(5):850–853.

9. Knobil E. The GnRH pulse generator. In: Delamarre-van de Waal HA, van Rees GP, Shoemaker J, Plant TM, eds. *In: Control of the Onset of Puberty III*. Amsterdam: Elsevier; 1989:11–20.

10. Collins TJ. The use of mouse pituitary fragments to study LH secretion. *Endocr Res*. 1990;16(1):107–133.

11. Karsch FJ, Bowen JM, Caraty A, Evans NP, Moenter SM. Gonadotropin-releasing hormone requirements for ovulation. *Biol.Reprod.* 1997;56:303–309.

12. Li XF, Kinsey-Jones JS, Cheng Y, et al. Kisspeptin Signalling in the Hypothalamic Arcuate Nucleus Regulates GnRH Pulse Generator Frequency in the Rat. *PLoS ONE*. 2009;4(12):e8334.

13. Belchetz P, Plant TM, Nakai Y, Keogh EJ, Knobil E. Hypophyseal responses to continuous and intermittent delivery of hypothalamic gonadotropin releasing hormone. *Science*. 1978;202:631–632.

14. Weiss JM, Jameson JL, Burrin M, Crowley WF. Divergent responses of gonadotropin subunit messenger RNAs to continuous versus pulsatile gonadotropin-releasing hormone in vitro. *Mol.Endocrinol.* 1990;4:557–564.

15. Knobil EN, Plant TM, Wildt L, Belchetz P, Marshall G. Control of the Rhesus Monkey Menstrual Cycle: Permissive Role of the Hypothalamic Gonadotropin-Releasing Hormone. *Science*. 1980;207(4437):1371–1373.

16. Cox NM, Britt JH. Effects of Estradiol on Hypothalamic GnRH and Pituitary and Serum LH and FSH in Ovariectomized Pigs. *Journal of Animal Science*. 1982;55:901–908.

17. Peterson SL, Ottem EN, Carpenter CD. Direct and Indirect regulation of gonadotropin-releasing hormone neurons by estradiol. *Biology of Reproduction*. 2003;69:8.

18. Johnson M. Positive and Negative Feeedback are Mediated at the Level of Both Hypothalamus and Pituitary. In: *Johnson and Everitt's Essential Reproduction*. 6th ed. Malden. MA: Blackwell Publishing; 2007:112–116.

19. Couse JF, Korach KS. Estrogen receptor null mice: what have we learned and where will they lead us? *Endocr Rev*. 1999;20(3):358–417.

20. Hewitt SC, Korach KS. Oestrogen receptor knockout mice: roles for oestrogen receptors alpha and beta in reproductive tissues. *Reproduction*. 2003;125(2):143–9.

21. Wintermantel TM, Elzer J, Herbison AE, Fritzemeier KH, Schutz G. Genetic dissection of estrogen receptor signaling in vivo. *Ernst Schering Found Symp Proc*. 2006;(1):25–44.

22. Ruf KB, Wilkinson M, de Ziegler D, Cassard D. Ovarian control of gonadotropin secretion during induced precocious sexual maturation in the rat. *Neuroendocrinology*. 1976;22(3):226–230.

23. Burger HG. Neuroendocrine Control of Human Ovulation. *Int J Fertil*. 1981;26(3):153–60.

24. Wun WS, Thorneycroft IH. Estradiol positive feedback on the rat anterior pituitary gland in vitro. *Mol Cell Endocrinol*. 1987;54(2-3):165–169.

25. Randall D, Burggren W, French K. Steroid Sex Hormones in Females. In: *Eckert Animal Physiology*. 5th ed. New York: W.H. Freeman and Company; 2002:345–348.

26. Erskine MS. Solicitation Behavior in th Estrous Rat: A Review. *Horm Behav*. 1989;23:473–502.

27. Hardy DF, DeBold J.F. The relationship between levels of exogenous hormones and the display of lordosis by the female rat. *Horm Behav*. 1971;2:287–297.

28. Miller G, Tybur JM, Jordan BD. Ovulatory Cycle Effects on Tip Earnings by Lap Dancer: Econimic Evidence for Human Estrus. *Evolution and Human Behavior*. 2007;28:375–381.

29. Klein DC, Moore RY, Reppert SM. *Suprachiasmatic nucleus. The minds clock*. (Klein DC, Moore RY, Reppert SM, eds.). New York: Oxford University Press; 1991. Available at: file://localhost/Users/horacio/Grants/Royalty/Research%20Plan.

30. Welsh DK, Logothetis DE, Meister M, Reppert SM. Individual neurons dissociated from rat suprachiasmatic nucleus express independently phased circadian firing rhythms. *Neuron*. 1995;14:697–706.

31. Balsalobre A, Damiola F, Schibler U. A serum shock induces circadian gene expression in mammalian tissue culture cells. *Cell*. 1998;93(6):929–37.

32. Hastings M, Reddy AB, Maywood ES. Timing in Brain and Periphery, in Health and Disease. *Nature Reviews Neuroscience*. 2003;4:649–661.

33. Dunlap JC. Molecular biology of circadian pacemaker systems. In: Dunlap JC, Loros JJ, DeCoursey PJ, eds. *Chronobiology: Biological Timekeeping*. Sunderland: Sinauer; 2004:213–253.

34. Tomita J, Nakajima M, Kondo T, Iwasaki H. No Transcription-Translation Feedback in Circadian Rhythm of KaiC Phosphorylation. *Science*. 2005;307:251–254.

35. Steeves TD, King DP, Zhao Y, et al. Molecular cloning and characterization of the human CLOCK gene: expression in the suprachiasmatic nuclei. *Genomics*. 1999;57(2):189–200.

36. Yoo SH, Yamazaki S, Lowrey PL, et al. PERIOD2::LUCIFERASE real-time reporting of circadian dynamics reveals persistent circadian oscillations in mouse peripheral tissues. *Proc Natl Acad Sci U S A*. 2004;101(15):5339–46.

37. Ko CH, Takahashi JS. Molecular components of the mammalian circadian clock. *Human molecular genetics*. 2006;15 Spec No 2:R271–7.

38. Duong H, Robles M, Knutti D, Weitz CJ. A molecular mechanism for circadian clock negative feedback. *Science*. 2011;332:1436–1439.

39. Kucera N, Schmalen I, Hennig S, et al. Unwinding the differences of the mammalian PERIOD clock proteins from crystal structure to cellular function. *Proc Natl Acad Sci USA*. 2012;109(9):3311–3316.

40. Meng QJ, Logunova L, Maywood ES, et al. Setting clock speed in mammals: The CK1 epsilon tau mutation in mice accelerates circadian pacemakers by selectively destabilizing PERIOD proteins. *Neuron*. 2008;58(1):78–88.

41. Aton SJ, Herzog ED. Come together, right...now: Synchronization of rhythms in a mammalian circadian clock. *Neuron*. 2005;48(4):531–534.

42. Aton SJ, Colwell CS, Harmar AJ, Waschek J, Herzog ED. Vasoactive intestinal polypeptide mediates circadian rhythmicity and synchrony in mammalian clock neurons. *Nat Neurosci*. 2005;8(4):476–83.

43. de Vries MJ, Nunes Cardozo B, van der Want J, de Wolf A, Meijer JH. Glutamate immunoreactivity in terminals of the retinohypothalamic tract of the brown Norwegian rat. *Brain Res*. 1993;612:231–237.

44. Fu YB, Zhong HN, Wang MHH, et al. Intrinsically photosensitive retinal ganglion cells detect light with a vitamin A-based photopigment, melanopsin. *Proceedings of the National Academy of Sciences of the United States of America*. 2005;102(29):10339–10344.

45. Guler AD, Ecker JL, Lall GS, et al. Melanopsin cells are the principal conduits for rod-cone input to non-image-forming vision. *Nature*. 2008;453(7191):102–U6.

46. Herzog ED, Geusz ME, Khalsa SBS, Straume M, Block GD. Circadian rhythms in mouse suprachiasmatic nucleus explants on multimicroelectrode plates. *Brain Res.* 1997;757:285–290.

47. Lewy AJ, Emens JS, Sack RL, Hasler BP, Bernert RA. Zeitgeber hierarchy in humans: resetting the circadian phase positions of blind people using melatonin. *Chronobiol Int*. 2003;20:837–852.

48. Yamazaki S, Numano R, Abe M, et al. Resetting central and peripheral circadian oscillators in transgenic rats. *Science*. 2000;288(5466):682–5.

49. Ikeda M, Sugiyama T, Wallace CS, et al. Circadian dynamics of cytosolic and nuclear Ca2+ in single suprachiasmatic nucleus neurons. *Neuron*. 2003;38:253–263.

50. Moore RY, Eichler VB. Loss of a circadian adrenal corticosterone rhythm following suprachiasmatic lesions in the rat. *Brain Research*. 1972;42:201–206.

51. Stephan FK, Zucker I. Circadian rhythms in drinking behavior and locomotor activity of rats are eliminated by hypothalamic lesions. *Proc.Natl.Acad.Sci.USA*. 1972;69:1583–1586.

52. Rusak B, Zucker I. Neural regulation of circadian rhythms. *Physiol Rev*. 1979;59(3):449–526.

53. Ralph MR, Foster RG, Davis FC, Menaker M. Transplanted suprachiasmatic nucleus determines circadian period. *Science*. 1990;247(4945):975–8.

54. Sawaki Y, Nihonmatsu I, Kawamura H. Transplantation of the neonatal suprachiasmatic nuclei into rats with complete bilateral suprachiasmatic lesions. *Neurosci.Res.* 1984;1:67–72.

55. Lehman MN, Silver R, Gladstone WR, et al. Circadian rhythmicity restored by neural transplant. Immunocytochemical characterization of the graft and its integration with the host brain. *J Neurosci*. 1987;7(6):1626–38.

56. DeCoursey PJ, Buggy J. Circadian rhythmicity after neural transplant to hamster third ventricle: specificity of suprachiasmatic nuclei. *Brain Res*. 1989;500(1-2):263–75.

57. Yamazaki S, Straume M, Tei H, et al. Effects of aging on central and peripheral mammalian clocks. *Proc Natl Acad Sci U S A*. 2002;99(16):10801–6.

58. Abe M, Herzog ED, Yamazaki S, et al. Circadian rhythms in isolated brain regions. *J Neurosci*. 2002;22(1):350–6.

59. Izumo M, Johnson CH, Yamazaki S. Circadian gene expression in mammalian fibroblasts revealed by real-time luminescence reporting: temperature compensation and damping. *Proc Natl Acad Sci U S A*. 2003;100(26):16089–94.

60. Filipski E, King VM, Etienne MC, et al. Persistent twenty-four hour changes in liver and bone marrow despite suprachiasmatic nuclei ablation in mice. *Am J Physiol Regul Integr Comp Physiol*. 2004;287(4):R844–51.

61. Nagoshi E, Saini C, Bauer C, et al. Circadian gene expression in individual fibroblasts; cell-autonomous and self-sustained oscillators pass time to daughter cells. *Cell*. 2004;119(5):693–705.

62. Ruan GX, Zhang DQ, Zhou T, Yamazaki S, McMahon DG. Circadian organization of the mammalian retina. *Proceedings of the National Academy of Sciences of the United States of America*. 2006;103(25):9703–8.

63. Leibetseder V, Humpeler S, Svoboda M, et al. Clock genes display rhythmic expression in human hearts. *Chronobiol Int*. 2009;26:621–636.

64. Meyers-Bernstein E, Jetton AE, Matsumo S, et al. Effects of suprachiasmatic transplants on circadian rhythms of neuroendocrine function in golden hamsters. *Endocrinology*. 1999;140:207–218.

65. Pendergast JS, Niswender KD, Yamazaki S. Tissue-specific function of Period3 in circadian rhythmicity. *PLoS ONE*. 2012;7(1).

66. Mazoccoli G, Pazienza V, Vinciguerra M. Clock Genes and Clock-Controlled Genes in the Regulation of Metabolic Rhythms. *Chronobiol.Int.* 2012;29(3):227–51.

67. Saini C, Morf J, Stratmann M, Gos P, Schibler U. Simulated body temperature rhythms reveal the phase-shifting behavior and plasticity of mammalian circadian oscillators. *Genes Dev*. 2012.

68. Lucas RJ, Stirland JA, Darrow JM, Menaker M, Loudon AS. Free running circadian rhythms of melatonin, luteinizing hormone, and cortisol in Syrian hamsters bearing the circadian tau mutation. *Endocrinology*. 1999;140(2):758–64.

69. Alleva JJ, Waleski MV, Alleva FR. A biological clock controlling the estrous cycle of the hamster. *Endocrinology*. 1971;88:1368–1379.

70. Stetson MH, Anderson PJ. Circadian pacemaker times gonadotropin release in free-running female hamsters. *Am J Physiol*. 1980;238(1):R23–7.

71. Moline ML, Albers HE, Todd RB, Moore-Ede MC. Light-dark entrainment of proestrous LH surges and circadian locomotor activity in female hamsters. *Horm Behav*. 1981;15(4):451–8.

72. Moline ML, Albers HE. Response of circadian locomotor activity and the proestrus luteinizing hormone surge to phase shifts of the light-dark cycle in the hamster. *Physiol.Behav.* 1988;43:435–440.

73. Fitzgerald K, Zucker I. Circadian organization of the estrous cycle of the golden hamster. *Proc Natl Acad Sci U S A*. 1976;73(8):2923–7.

74. Coen CW, MacKinnon PC. Lesions of the suprachiasmatic nuclei and the serotonin-dependent phasic release of luteinizing hormone in the rat: effects on drinking rhythmicity and on the consequences of preoptic area stimulation. *J Endocrinol*. 1980;84:231–236.

75. Palm IF, Van Der Beek EM, Wiegant VM, Buijs RM, Kalsbeek A. Vasopressin induces a luteinizing hormone surge in ovariectomized, estradiol-treated rats with lesions of the suprachiasmatic nucleus. *Neuroscience*. 1999;93(2):659–66.

76. Cahill DJ, Wardle PG, Harlow CR, Hull MG. Onset of the preovulatory luteinizing hormone surge: diurnal timing and critical follicular prerequisites. *Fertil Steril*. 1998;70(1):56–9.

77. Edwards R. Test-tube babies, 1981. *Nature*. 1981;(293):253–256.

78. Labyak SE, Lava S, Turek F, Zee PC. Effects of shiftwork on sleep and menstrual function in nurses. *Health Care Women Int*. 2002;23:703–714.

79. Knutsson A. Health disorders of shift workers. *Occupational medicine (Oxford, England)*. 2003;53(2):103–8.

80. Schernhammer ES, Laden F, Speizer FE, et al. Night-shift work and risk of colorectal cancer in the nurses' health study. *J Natl Cancer Inst*. 2003;95(11):825–8.

81. Gottsch ML, Cunningham MJ, Smith JT, et al. A role for kisspeptins in the regulation of gonadotropin secretion in the mouse. *Endocrinology*. 2004;145(9):4073–7.

82. Shahab M, Mastronardi C, Seminara SB, et al. Increased hypothalamic GPR54 signaling: a potential mechanism for initiation of puberty in primates. *Proc Natl Acad Sci USA*. 2005;102:2129–2134.

83. Clarkson J, Herbison AE. Postnatal development of kisspeptin neurons in mouse hypothalamus; sexual dimorphism and projections to gonadotropin-releasing hormone neurons. *Endocrinology*. 2006;147(12):5817–25.

84. Franceschini I, Lomet D, Cateau M, et al. Kisspeptin immunoreactive cells of the ovine preoptic area and arcuate nucleus co-express estrogen receptor alpha. *Neurosci Lett*. 2006;401:225–230.

85. Rometo AM, Krajewski SJ, Voytko ML, Rance NE. Hypertrophy and increased kisspeptin gene expression in the hypothalamic infundibular nucleus of postmenopausal women and ovariectomized monkeys. *J Clin Endocrinol Metab*. 2007;92:2744–2750.

86. Smith JT, Clay CM, Caraty A, Clarke IJ. KiSS-1 messenger ribonucleic acid expression in the hypothalamus of the ewe is regulated by sex steroids and season. 148: 1150–1157, 2007. *Endocrinology*. 2007;48:1150–1157.

87. Clarkson J, d' Anglemont de Tassigny X, Moreno AS, Colledge WH, Herbison AE. Kisspeptin-GPR54 signaling is essential for preovulatory gonadotropin-releasing hormone neuron activation and the luteinizing hormone surge. *J Neurosci*. 2008;28(35):8691–7.

88. Clarkson J, d' Anglemont de Tassigny X, Colledge WH, Herbison AE. Distribution of kisspeptin neurones in the adult female mouse brain. *J Neuroendocrinol*. 2009;21:673–682.

89. Popa SM, Clifton DK, Steiner RA. The role of kisspeptins and GPR54 in the neuroendocrine regulation of reproduction. *Annu Rev Physiol*. 2008;70:213–238.

90. Matsui H, Takatsu Y, Kumano S, Matsumoto H, Ohtaki T. Peripheral Administration of Metastin Induces Marked Gonadotropin Release and Ovulation in the Rat. *Beiochemical and Biophysical Research Communications*. 2004;320(2):383–388.

91. Navarro VM, Castellano JM, Fernandez-Fernandez R, et al. Developmental and hormonally regulated messenger ribonucleic acid expression of KiSS-1 and its putative receptor, GPR54, in rat hypothalamus

and potent luteinizing hormone-releasing activity of KiSS-1 peptide. *Endocrinology*. 2004;145:4565–4574.

92. Thompson EL, Patterson M, Murphy KG, et al. Central and peripheral administration of kisspeptin-10 stimulates the hypothalamic-pituitary-gonadal axis. *J Neuroendocrinol*. 2004;16(10):850–8.

93. Dhillo WS, Chaudhri OB, Patterson M, et al. Kisspeptin-54 stimulates the hypothalamic-pituitary gonadal axis in human males. *Clin Endocrinol Metab*. 2005;90:6609–6615.

94. Messager S, Chatzidaki EE, Ma D, et al. Kisspeptin directly stimulates gonadotropin releasing hormone release via G protein-coupled receptor 54. *Proc Natl Acad Sci USA*. 2005;102:1761–1766.

95. Han SK, Gottsch ML, Lee KJ, et al. Activation of gonadotropin-releasing hormone neurons by kisspeptin as a neuroendocrine switch for the onset of puberty. *J Neurosci*. 2005;25:11349–11356.

96. Goodman RL. Goodman RL (1996) Neural systems mediating the negative feedback actions of estradiol and progesterone in the ewe. Acta Neurobiol Exp (Wars) 56:727–741. *Acta Neurobiol Exp*. 56:727–741.

97. Thind KK, Goldsmith PC. Thind KK, Goldsmith PC (1988) Infundibular gonadotropin-releasing hormone neurons are inhibited by direct opioid and autoregulatory synapses in juvenile monkeys. Neuroendocrinology 47:203–216. *Neuroendocrinology*. 47:203–216.

98. Nishihara M, Matsukawa T, Kimura F. Responses of arcuate neurons to some putative neurotransmitters in perfused rat hypothalamic slices: effects of in vivo and in vitro estrogen treatments. *Jpn J Physiol*. 1986;36:683–697.

99. Wiegand SJ, Terasawa E, Bridson WE. Persistent estrus and blockade of progesterone-induced LH release follows lesions which do not damage the suprachiasmatic nucleus. *Endocrinology*. 1978;102(5):1645–8.

100. Terasawa E, Wiegand SJ, Bridson WE. A role of medial preoptic nucleus on afternoon of proestrus in female rats. *Am.J.Physiol.* 1980;238:E533–E539.

101. Popolow HB, King JC, Gerall AA. Rostral medial preoptic area lesions' influence on female estrous processes and LHRH distribution. *Physiol.Behav.* 1981;27:855–861.

102. Simerly RB, Chang C, Muramatsu M, Swanson LW. Distribution of androgen and estrogen receptor mRNA-containing cells in the rat brain: an in sity hybridization study. *J.Comp.Neurol.* 1990;294:76–95.

103. Gu GB, Simerly RB. Projections of the sexually dimorphic anteroventral periventricular nucleus in the female rat. *J Comp Neurol*. 1997;384(1):142–64.

104. Polston EK, Simerly RB. Ontogeny of the projections from the anteroventral periventricular nucleus of the hypothalamus in the female rat. *J Comp Neurol*. 2006;495:122–132.

105. Gottsch ML, Navarro VM, Zhao Z, et al. Regulation of KIss1 and Dynorphin Gene Expression in the Murine Brain by Classical and Nonclassical Estrogen Receptor Pathways. *J Neurosci*. 2009;29(29):9390–9395.

106. Smith JT, Cunningham MJ, Rissman EF, Clifton DK, Steiner RA. Regulation of Kiss1 gene expression in the brain of the female mouse. *Endocrinology*. 2005;146(9):3686–92.

107. Burke MC, Letts PA, Krajewski SJ, Rance NE. Coexpression of dynorphin and neurokinin B immunoreactivity in the rat hypothalamus: morphologic evidence of interrelated function within the arcuate nucleus. *J Comp Neurol*. 2006;498:712–726.

108. Goodman RL, Lehman MN, Smith JT, et al. Kisspeptin neurons in the arcuate nucleus of the ewe express both dynorphin A and neurokinin B. *Endocrinology*. 2007;148:5752–5760.

109. Navarro VM, Gottsch ML, Chavkin CC, et al. Regulation of gonadotropin- releasing hormone secretion by kisspeptin/ dynorphin/neurokinin B neurons in the arcuate nucleus of the mouse. J Neurosci 29: 11859–11866, 2009. *J Neurosci*. 2009;29:11859–11866.

110. Kinsey-Jones JS, Grachev P, Li XF, et al. The inhibitory effects of neurokinin B on GnRH pulse generator frequency in the female rat. *Endocrinology*. 2012;153(1):307–315.

111. Schulz R, Wilhelm A, Pirke KM, Gramsch C, Herz A. Beta-endorphin and dynorphin control serum luteinizing hormone level in immature female rats. *Nature*. 1981;294:757–759.

112. Kinoshita F, Nakai Y, Katakami H, Imura H. Suppressive effect of dynorphin-(1-13) on luteinizing hormone release in conscious castrated rats. Life Sci 30: 1915–1919, 1982. *Life Sci*. 1982;30:1915–1919.

113. Sandoval-Guzman T, Rance NE. Central injection of senktide, an NK3 receptor agonist, or neuropeptide Y inhibits LH secretion and induces different patterns of Fos expression in the rat hypothalamus. *Brain Res*. 2004;1026:307–312.

114. Krajewski SJ, Anderson MJ, Iles-Shih L, et al. Krajewski SJ, Anderson MJ, Iles-Shih L, Chen KJ, Urbanski HF, Rance NE. Morphologic evidence that neurokinin B modulates gonadotropin-releasing hormone secretion via neurokinin 3 receptors in the rat median eminence. J Comp Neurol 489: 372–386, 2005. *J Comp Neurol*. 2005;489:372–386.

115. Ramaswamy S, Guerriero KA, Gibbs RB, Plant TM. Structural interactions between kisspeptin and GnRH neurons in the mediobasal hypothalamus of the male rhesus monkey (Macaca mulatta) as revealed by double immunofluorescence and confocal microscopy. *Endocrinology*. 2008;149:4387–4395.

116. Desroziers E, Mikkelsen J, Simonneaux V, et al. Mapping of Kisspeptin Fibres in the BRain of the Pro-Oestrous Rat. *J Neuroendocrinol*. 2010;22:1101–1112.

117. Krajewski SJ, Burke MC, Anderson MJ, McMullen NT, Rance NE. Forebrain projections of arcuate neurokinin B neurons demonstrated by anterograde tract-tracing and monosodium glutamate lesions in the rat. *Neuroscience*. 2009;166:680–697.

118. d' Anglemont de Tassigny X, Colledge WH. The role of Kisspeptin in Signaling in Reproduction. *Physiology*. 2010;25:207–217.

119. Plant TM, Krey LC, Moossy J, et al. The arcuate nucleus and the control of gonadotropin and prolactin secretion in the female rhesus monkey (Macaca mulatta). *Endocrinology*. 1978;102(1):52–62.

120. Simberly R, Swanson LW, Gorski RA. The distribution of monoaminergic cells and fibers in a periventricular preoptic nucleus involved in the control of gonadotropin release: immunohistochemical evidence for a dopaminergic sexual dimorphism. *Brain Res*. 1985;330:55–64.

121. Simberly R, Swanson LW, Handa RJ, Gorski RA. Simerly RB, Swanson LW, Handa RJ, Gorski RA. Influence of perinatal androgen on the sexually dimorphic distribution of tyrosine hydroxylaseimmunoreactive cells and fibers in the anteroventral periventricular nucleus of the rat. Neuroendocrinology 40: 501–510, 1985. *Neuroendocrinology*. 1985;40:501–510.

122. Kauffman AS, Gottsch ML, Roa J, et al. Sexual differentiation of Kiss1 gene expression in the brain of the rat. *Endocrinology*. 2007;148(4):1774–1783.

123. Takase K, Uenoyama Y, Inoue N, et al. Possible role of oestrogen in pubertal increase of Kiss1/kisspeptin expression in discrete hypothalamic areas of female rats. *J Neuroendocrinol*. 2009;21:527–537.

124. Kinoshita M, Tsukamura H, Adachi S, et al. Involvement of central metastin in the regulation of preovulatory luteinizing hormone surge and estrous cyclicity in female rats. *Endocrinology*. 2005;146:4431–4436.

125. Robertson J, Clifton DK, De La Iglesia HO, Steiner RA, Kauffman AS. Circadian Regulation of Kiss1 Neurons: Implications for Timing the Preovulatory GnRH/LH Surge. *Endocrinology*. 2009;150:3664–3671.

126. Brailoiu GC, Dun SL, Ohsawa M, et al. KiSS-1 expression and metastin-like immunoreactivity in the rat brain. *J Comp Neurol*. 2005;481(3):314–29.

127. Irwig MS, Fraley GS, Smith JT, et al. Kisspeptin Activation of Gonadotropin Releasing Hormone Neurons and Regulation of KiSS-1 mRNA in the Male Rat. *Neuroendocrinology*. 2005;80(4):264–272.

128. de Roux N, Genin E, Carel JC, et al. Hypogonadotropic hypogonadism due to loss of function of the KiSS1-derived peptide receptor GPR54. *Proc Natl Acad Sci USA*. 2003;100:10972–10976.

129. Seminara SB, Messager S, Chatzidaki EE, et al. The GPR54 gene as a regulator of puberty. *N Engl J Med*. 2003;349:1614–1627.

130. Lapatto R, Pallais JC, Zhang D, et al. Kiss1-/- mice exhibit more variable hypogonadism than Gpr54-/- mice. *Endocrinology*. 2007;148:4927–4936.

131. Seminara SB, Crowley WF. Kisspeptin and GPR54: discovery of a novel pathway in reproduction. *J Neuroendocrinol*. 2008;20:727–731.

132. de la Iglesia HO, Cambras T, Schwartz WJ, Diez-Noguera A. Forced Desynchronization of Dual Circadian Oscillators within the Rat Suprachiasmatic Nucleus. *Curr Biol*. 2004;14(9):796–800.

133. Schwartz MD, Wotus C, Liu T, et al. Schwartz MD, Wotus C, Liu T, Friesen WO, Borjigin J, Oda GA, de la Iglesia HO 2009 Dissociation of circadian and light inhibition of melatonin release through forced desynchronization in the rat. Proc Natl Acad Sci U S A 106:17540-17545. *Proc Natl Acad Sci USA*. 2009;106:17540–17545.

134. Moore RY, Speh JC, Leak RK. Suprachiasmatic nucleus organization. *Cell Tissue Res*. 2002;309(1):89–98.

135. Watson RE, Langub MC. Vasopressinergic synaptic input upon estrogen receptive neurons in the anterior preoptic region of the rat: suprachiasmatic nucleus origin? *Soc.Neurosci.Abstr.* 1992;18:53.5–0.

136. de la Iglesia HO, Blaustein JD, Bittman EL. The suprachiasmatic area in the female hamster projects to neurons containing estrogen receptors and GnRH. *Neuroreport*. 1995;6(13):1715–22.

137. Van der Beek EM, Horvath TL, Wiegant VM, van den Hurk R, Buijs RM. Evidence for a direct neuronal pathway from the suprachiasmatic nucleus to the gonadotropin-releasing hormone system: combined tracing and light and electron microscopic immunocytochemical studies. *J Comp Neurol*. 1997;384(4):569–79.

138. Ma Y., Kelly MJ, Ronnekleiv OK. Pro-gonadotropin-releasing hormone (ProGnRH) and GnRH content in the preoptic area and the basal hypothalamus of anterior medial preoptic area nucleus/suprachiasmatic nucleus-lesioned persistent estrous rats. *Endocrinology*. 1990;127:2654–2664.

139. Miller BH, Olson SL, Levine JE, et al. Vasopressin regulation of the proestrous luteinizing hormone surge in wild-type and Clock mutant mice. *Biol Reprod*. 2006;75(5):778–84.

140. Christian CA, Moenter SM. Vasoactive Intestinal Polpeptide Can Excite Gonadotropin-Releasing Hormone Neurons in a Manner Dependent on Estradiol and Gated by Time of Day. *Endocrinology*. 2008;149(6):3130–3136.

141. van der Beek EM, van Oudheusden HJ, Buijs RM, et al. Preferential induction of c-fos immunoreactivity in vasoactive intestinal polypeptide-innervated gonadotropin-releasing hormone neurons during a steroid-induced luteinizing hormone surge in the female rat. *Endocrinology*. 1994;134(6):2636–44.

142. Harney JP, Scarbrough K, Rosewell KL, Wise PM. In vivo antisense antagonism of vasoactive intestinal peptide in the suprachiasmatic nuclei causes aging-like changes in the estradiol-induced luteinizing hormone and prolactin surges. *Endocrinology*. 1996;137(9):3696–701.

143. Gerhold LM, Rosewell KL, Wise PM. Suppression of vasoactive intestinal polypeptide in the suprachiasmatic nucleus leads to aging-like alterations in cAMP rhythms and activation of gonadotropin-releasing hormone neurons. *J Neurosci*. 2005;25(1):62–7.

144. Smarr B, Morris E, de la Iglesia H. The Dorsomedial Suprachiasmatic Nucleus Times Circadian Expression of Kiss1 and the Luteinizing Hormone Surge. *Endocrinology*. 2012;153(6).

145. Lee ML, Weller JR, Cambras T, de la Iglesia HO. Forced desynchronization of REM and nonREM sleep in the rat. *Society for Research on Biological Rhythms abstract*. 2006.

146. van der Beek EM, Wiegant VM, van der Donk HA, van den Hurk R, Buijs RM. Lesions of the suprachiasmatic nucleus indicate the presence of a direct vasoactive intestinal polypeptide-containing projection to gonadotrophin-releasing hormone neurons in the female rat. *J Neuroendocrinol*. 1993;5(2):137–44.

147. Card JP, Brecha N, Karten HJ, Moore RY. Immunocytochemical localization of vasoactive intestinal polypeptide-containing cells and processes in the suprachiasmatic nucleus of the rat: light and electron microscopic analysis. *J Neurosci*. 1981;1(11):1289–303.

148. Chappell PE. Clocks and the black box: Circadian influences on gonadotropin-releasing hormone secretion. *Journal of Neuroendocrinology*. 2005;17(2):119–130.

149. de la Iglesia HO, Schwartz WJ. Timely ovulation: Circadian regulation of the female hypothalamo-pituitary-gonadal axis. *Endocrinology*. 2006;147(3):1148–1153.

150. Sellix MT, Menaker M. Circadian clocks in the ovary. *Trends Endocrinol Metab*. 2010;21:628–636.

151. Williams WP 3rd, Jarjisian SG, Mikkelsen JD, Kreigsfeld LJ. Circadian control of kisspeptin and a gated GnRH response mediate the preovulatory luteinizing hormone surge. *Endocrinology*. 2010;152:595–606.

152. Gibson EM, Humber SA, Jain S, et al. Alterations in RFamide-related peptide expression are coordinated with the preovulatory luteinizing hormone surge. *Endocrinology*. 2008;149:4958–4969.

153. Hickok JR, Tischkau SA. In vivo circadian rhythms in gonadotropin-releasing hormone neurons. *Neuroendocrinology*. 2010;91:110–120.

154. Palm IF, van der Beek EM, Wiegant VM, Buijs RM, Kalsbeek A. The stimulatory effect of vasopressin on the luteinizing hormone surge in ovariectomized, estradiol-treated rats is time-dependent. *Brain Res*. 2001;901(1-2):109–16.

155. Funabashi T, Shinohara K, Mitsushima D, Kimura F. Gonadotropin-releasing hormone exhibits circadian rhythm in phase with arginine-vasopressin in co-cultures of the female rat preoptic area and suprachiasmatic nucleus. *J Neuroendocrinol*. 2000;12(6):521–8.

156. Funabashi T, Aiba S, Sano A, Shinohara K, Kimura F. Intracerebroventricular injection of arginine-vasopressin V1 receptor antagonist attenuates the surge of luteinizing hormone and prolactin secretion in proestrous rats. *Neurosci Lett*. 1999;260:37–40.

157. Kalamatianos T, Kallo I, Goubillon ML, Coen CW. Cellular expression of V1a vasopressin receptor mRNA in the female rat preoptic area: effects of oestrogen. *J Neuroendocrinol*. 2004;16(6):525–33.

158. Mahoney MM, Smale L. Arginine vasopressin and vasoactive intestinal polypeptide fibers make appositions with gonadotropin-releasing hormone and estrogen receptor cells in the diurnal rodent Arvicanthis niloticus. *Brain Res*. 2005;1049(2):156–64.

159. Vida B, Deli L, Hrabovszky E, et al. Evidence for suprachiasmatic vasopressin neurones innervating kisspeptin neurones in the rostral periventricular area of the mouse brain: regulation by oestrogen. *J Neuroendocrinol*. 2010;22:1032–1039.

160. Smith MJ, Jiennes L, Wise PM. Localization of the VIP2 receptor protein on GnRH neurons in the female rat. *Endocrinology*. 2000;141(11):4317–20.

161. Vijayan E, Samson WK, Said SI, McCann SM. Vasoactive intestinal peptide: evidence for a hypothalamic site of action to release growth hormone, luteinizing hormone, and prolactin in conscious ovariectomized rats. *Endocrinology*. 1979;104:53–57.

162. Samson WK, Burton KP, Reeves JP, McCann SM. Vasoactive intestinal peptide stimulates luteinizing hormone-releasing hormone release from median eminence synaptosomes. *Regul Pept*. 1981;2:253–264.

163. Weick RF, Stobie KM. Vasoactive intestinal peptide inhibits the steroid-induced LH surge in the ovariectomized rat. *J.Endocr.* 1992;133:433–437.

164. van der Beek EM, Swarts HJ, Wiegant VM. Central administration of antiserum to vasoactive intestinal peptide delays and reduces luteinizing hormone and prolactin surges in ovariectomized, estrogen-treated rats. *Neuroendocrinology*. 1999;69(4):227–37.

165. Stobie KM, Weick RF. Vasoactive intestinal peptide inhibits luteinizing hormone secretion: the inhibition is not mediated by dopamine. *Neuroendocrinology*. 1989;49:597–603.

166. Alexander MJ, Clifton DK, Steiner RA. Vasoactive intestinal polypeptide effects a central inhibition of pulsatile luteinizing hormone secretion in ovariectomized rats. *Endocrinology*. 1985;117:2134–2139.

167. Everett JW, Sawyer CH. A 24-hour periodicity in the “LH-release apparatus” of female rats, disclosed by barbiturate sedation. *Endocrinology*. 1950;47:198–218.

168. Haus E, Smolensky M. Biological clocks and shift work: Circadian dysregulation and potential long-term effects. *Cancer Causes & Control*. 2006;17(4):489–500.

169. Sack RL, Blood ML, Lewy AJ. Melatonin Rhythms in Night Shift Workers. *Sleep*. 1992;15:434–441.

170. Cambras T, Weller JR, Angles-Pujoras M, et al. Circadian desynchronization of core body temperature and sleep stages in the rat. *Proceedings of the National Academy of Sciences of the United States of America*. 2007;104(18):7634–9.

171. Lee ML, Swanson BE, de la Iglesia HO. Circadian Timing of REM Sleep is coupled to an oscillator within the dorsomedial suprachiasmatic nucleus. *Curr Biol*. 2009;19:848–852.

172. de la Iglesia HO. In situ hybridization of suprachiasmatic nucleus slices. In: Rosato E, ed. *Methods Mol Biol*. Humana Press; 2007:513–31. Available at: http://www.ncbi.nlm.nih.gov/entrez/query.fcgi?cmd=Retrieve&db=PubMed&dopt=Citation&list_uids=17417038.

Materials and Methods

Animals

Adult female Wistar rats, purchased from Charles River, were used for all the experiments. All experiments were performed according to the NIH Guide for Care and Use of Laboratory Animals and were approved by the University of Washington Institutional Animal Care and Use Committee.

Activity Cycles and Internal Desynchronization

Animal activity monitoring and internal desynchronization was carried out as reported previously[132]. Briefly, animals were singly housed either under a 12:12 light-dark cycle (LD24 control animals) or an 11:11 LD cycle (LD22 animals) with 50-150 lux light during the light phase and red light not brighter than 1 lux during the dark phase. LD22 animals were housed under 11:11 for 1-2 months. Locomotor activity was recorded using 2 perpendicular infrared beams crossed through the center of the cage, ~2 cm above the bedding, with beam breaks recorded digitally with ClockLab (Actimetrics, Wilmette, IL). Analysis of activity was carried out using the software El Temps‖(Dr. Antoni Díez-Noguera, University of Barcelona) and the graphs were imported into Adobe Photoshop to prepare final figures. Only LD22 animals showing 2 statistically-significant rhythms using periodogram analysis were used for any analysis. Assessment of alignment and misalignment during the forced desynchrony protocol was done by eye fitting onset-timing lines of the two rhythms found under periodogram analysis, as shown in Fig. 3.2, by at least two independent researchers. Significantly desynchronized animals were grouped into either aligned or misaligned groups for blood and tissue collection,

but this did not change their housing or handling, only the time of collection relative to their activity cycles.

SCN lesions

Unilateral SCN lesions were carried out in a stereotaxic apparatus under isoflurane anesthesia. The skin over the cranium was sterilized and cut down the middle with a scalpel. Bregma and lamda were visualized and placed on the same on the same horizontal plane. A small hole was drilled in the skull and electrodes (size 00 insect pins coated with nail sealant except for the very tip) lowered at a 10º angle. Coordinates from bregma were: -0.9 mm rostrocaudal, 2.25 mm mediolateral and -9.5 mm dorsoventral. The lesion was made by application of a 1-mA AC current for 10 sec. The electrode was then removed, the skull sealed with gel-foam and the skin stapled with wound clips. Surgery was preceded by and followed every 12 h for 2 days by 0.05 mg buprenorphine/kg subcutaneous injections to minimize post-operative pain. All SCNX animals underwent ovariectomy while under anesthesia from the SCNX operation. Animals with lesions were sacrificed between 1 and 0 h before lights-off. For the purpose of grouping animals as successful or missed lesions, 16-µm brain sections were collected, stained with DAPI and the extent of the lesion assessed. Under DAPI staining, the SCN is revealed as a very discrete cluster of nuclei easily recognizable from the surrounding tissue. Lesions were rated successful if (1) the SCN ispilateral to the lesion side was ablated in at least 60% by area of the whole rostro-caudal extent of the nucleus; (2) there was no damage on the contralateral-side SCN throughout its rostro-caudal extent; and (3) the lesion did not extend into either the ipsi- or contralateral MPO and AVPV. Animals with ipsilateral SCN ablation below 60% were not

included in the study; animals in which lesions fell outside the SCN but not in the MPO or AVPV were counted as missed lesions.

Ovariectomy, E2 treatment, and catheterization

All ovariectomies were carried out under isoflurane anesthesia, using buprenorphine as indicated above. Internal incisions were closed with biodegradable suture while skin was closed with wound clips. Animals were allowed to heal at least two weeks. Two days before sacrifice, E_2-treated animals were implanted with 1cm x 1.57 mm internal diameter, 3.18mm outer diameter silastic capsules filled with 20% E_2/80% cholesterol by mass, and capped with silastic glue. This capsule size and concentration has been shown to yield 1.5-2 times the physiological concentration of E_2 during proestrus in rats[75]. Capsules were soaked overnight in 70% EtOH before being subcutaneously implanted into OVX rats under isoflurane anesthesia. Animals used for LH-profile generation were implanted with silastic catheters at the same time as E_2 implantation. The jugular vein was exposed and raised from the tissue, nicked but not severed, and silastic tubing with an internal diameter of 0.51 mm, 150 outer diameter of 0.94 mm, was inserted 4.3 cm, with its tip in the atrium. The catheter was anchored by suturing, threaded under the skin, extruded through the back of the neck, filled with 20u heparin and 120ug gentamicin/ml saline and plugged until bleeding.

Tissue collection

For LH profiles, hourly blood samples (0.12 ml) were collected through the implanted catheters. Blood volume was replaced with 35ºC saline, and the catheter refilled with heparinized saline. Bleeding and volume replacement took less than 3 min per animal, from the time of removing the cage from its rack to the time of returning it. Samples were then centrifuged at 4ºC, 1500

rpm, for 15 min. Plasma was separated and stored at -80º for processing by radioimmunoassay (RIA). For circadian sampling of mRNAs within brain tissue, brains were collected every 6 h, with predicted-peak time selected based on the *Kiss1* profile found previously in mice[125]. All animals were sacrificed by decapitation. Brains were collected immediately and frozen in -30ºC methyl butane; 1 ml of trunk blood was collected into centrifuge tubes with 20ul heparin (10,000 u/ml) and centrifuged as above. Plasma and brains were then stored at -80ºC until processed. All brains were cut into 16-µm sections in a cryostat, mounted on slides and frozen until histological processing.

Immunolabeling of cFOS and GnRH

Between 18 and 24 slices were stained for cFos and GnRH per animal, spanning the whole rostro-caudal extent of the MPO. Anti-GnRH antibody (FL-92, Santa Cruz Biotechnology, Santa Cruz, CA) diluted 1:400 and anti-cFOS antibody (SC-52, Santa Cruz Biotechnology) diluted 1:400 were used as primary antibodies. Secondary antibodies were Alexafluor 594 donkey anti-rabbit (Invitrogen, Grand Island, NY, #A10042) and FITC donkey anti-rabbit (Santa Cruz Biotechnology #SC-2090). Immunohistochemical labeling was done by fixing tissue in fresh 4% paraformaldehyde in phosphate buffer for 5 min, rinsing 3x5 min in phosphate-buffered saline (PBS), then blocking 30 min in PBS with 5% bovine serum albumin, 0.5% Triton X-100, 3% normal donkey serum, and 0.3% H_2O_2. Tissue was then incubated overnight at 4ºC with anti-cFOS in a 1:10 dilution of the blocking buffer, rinsed 3x5 min with PBS, incubated in FITC 1:400 for 2 h, rinsed 3x5 min in PBS, re-blocked and stained as before but with anti-GnRH antibody and Alexafluor 594 secondary antibody. The resulting tissue, though using two rabbit primary antibodies, could be scanned for GnRH cells labeled with Alexafluor 594, and the nuclear fill by

cFOS could then be checked by assessing FITC. Because GnRH is cytoplasmic and cFOS nuclear, cross-reactivity was not a problem as long as cFOS was labeled first. Slides were cover-slipped with Vectashield with DAPI (Vector Laboratories, Burlingame, CA, #H-1200). All slides stained for GnRH were scored in random order by two researchers blinded to the condition of the lesion. GnRH cells on both sides of the brain were counted as with or without cFOS staining under a fluorescent microscope. All scored slices for each individual were counted and summed, and the percentage of GnRH+ cells that contained a cFOS+ nucleus was quantified on each side of the brain. To assess any side-to-side cFOS expression asymmetry, separate paired Student t-tests were done for successful- and missed-lesion animals. Cell counting and lesion assessment was done on a Nikon microphot-FXA fluorescence light microscope. Photomicrographs were captured using a Leica SP5 confocal microscope.

In situ hybridization for *Kiss1* mRNA

In situ hybridization (ISH) was carried out as described previously[172]. Briefly, ^{35}S-labeled riboprobe was transcribed from a mouse *Kiss1* template[125], rPer1 template[132], or from template generated by PCR reaction from rat-liver DNA extracts using the following primers: forward (binds 537-560) of 5'- CGGTCGCCTTCTTCCAAGTATTAC -3; reverse (binds 1106-1085) of 5'- AAATGCTCTTCACGCTGCTGAC -3'. Fresh PCR products were ligated into Invitrogen pCR II vector (Invitrogen, Grand Island, NY, product # 46-0115) with the Invitrogen Dual Promoter TA Cloning Kit (Invitrogen, Grand Island, NY, product # 45-0007) and the resulting plasmids were then cloned into chemically competent E.coli “TOP10 cells” (Invitrogen, Grand Island, NY, product #C303006). Probe was amplified using Maxiprep protocol from Qiagen (Qiagen Inc., Valencia, CA, USA, product # 12162). After prehybridization washes, slides were incubated overnight at

52ºC with probe ($4*10^7$ cpm/ml). After posthybridization washes and dehydration in an alcohol series, they were air-dried to autoradiographic films for 4 days. All slides stained for *Kiss1* were scored masked to the experimental condition. *Kiss1* staining was scored by assigning each slice an area value based on the whole AVPV stained area above a preset darkness threshold and multiplying that area by the average optical density within that area. Each animal's score was the mean of the three strongest stained slices. For unilaterally lesioned animals, averages for both the ipsi- and contralateral sides of the lesion were calculated. To assess any side-to-side *Kiss1* expression asymmetry, separate paired Student t-tests were done for successful- and missed-lesion animals. All scores are reported as a percentage of the average score of the highest-scoring condition within the groups being compared. Two-way ANOVA was used for experiments with multiple factors (treatment and time). Tukey tests were then used for post-hoc analysis.

LH Radioimmunoassay

All LH RIAs were run with a probe that was iodinated in-house. Rat LH and antibodies were ordered from Dr. Parlow at the National Hormone and Pituitary Program (Harbor-UCLA Med Ctr., Torrance, CA), and iodinated with ^{125}I (Perkin Elmer, Waltham, MA, #016303401). Plasma from animals was mixed with RIA buffer (0.05M NaH2PO4, 0.25M Na2HPO4, 0.025M EDTA, 0.1% Triton X-100, 0.02% Trasylol protease inhibitor, 0.25% bovine serum albumin) and incubated with rabbit anti-rat-LH overnight at 4ºC. The next day, ^{125}I-LH was added, mixed, and incubated overnight. Finally, goat anti-rabbit IgG and normal rabbit serum were added, mixed, and incubated for 4 h. Separation buffer (as RIA buffer but 2.5% BSA, no Triton X-100 or Trasylol) was then added and all tubes were centrifuged. The supernatant was aspirated and

discarded and the pellet counted in a gamma counter. All steps were carried out at 4ºC. Samples were run in duplicates and serial dilutions of rat LH standard were used to create standard curves. Non-specific-binding was subtracted from all readings and 0-binding controls were used to calculate the final standard curve equation. All samples were assayed in two assays, with 3 standard curves per assay. The inter-assay variability was 3.5% and intra-assay variabilities were respectively 1.9% and 2.2%. The assay was sensitive between 0.5 and 16ng/ml. Values above these limits were brought to the maximum sensitivity; values below this limit were unchanged.

Rayleigh Statistics

To assess the clustering of LH surges, we used the Rayleigh test for circular distribution. Each LH onset time, defined as the first point to exceed five times the standard deviation of the lowest six points and to be contiguous with at least two other points also meeting this criterion, was converted into a circular phase with 360º equal to the relevant period (22 h, 24 h, or that animal‘s LD-dissociated period, usually ~25 h). Rayleigh statistics were then computed for each animal group (LD24, n = 7; LD22, n = 10 on aligned days, n = 9 on misaligned days) and relative to 24 h (for LD24 animals), and to 22 h or ~25 h (for LD22 animals). Alpha value was always set to 0.05. From the calculated statistics, the Rayleigh data was plotted using quantitative transformation of vectors in Adobe Photoshop.

Acknowledgements

There are a great number of people without whom I could not have done this work, and I do not have space here to praise every friend, mentor, teacher, coworker, classmate, and family member who has influenced me to want and be able to approach my Ph.D. at the University of Washington. I will try to truncate my commentary to contain only those at Seattle, but it will still be a long way from complete.

First of all I must thank my mentor and advisor, Dr. Horacio de la Iglesia. Since meeting him when I was at the UW interviewing for the program, it was clear that he was intelligent and excited, but also human. I have liked Horacio since I met him, and never once through the various ups and downs of my time in his lab have I regretted my decision to join his lab.

Horacio keeps an open door than I have probably abused at times. He has shown a willingness to sacrifice his continuity of thought for my experimental, teaching, or sometimes existential concerns. I thank him for this. In addition however, it reinforced in me a sense that my thoughts and concerns were valued in the work of the lab. That I took these feelings and channeled them into more independent pursuit of meaningful experiments and funding opportunities – several of each of which have proven fruitful – I hope is also a repayment to him, and encourages him to continue his generous stance.

I also must thank my committee not just for their official help, but for their advice in many things. Robert Steiner and Donald Clifton have provided an introduction to endocrinology which has helped me understand how to approach the questions I ask in this dissertation with far more clarity than my many text books on the subject have ever given me. In addition, they have provided a great deal of technical advice in the pursuit of better Kisspeptin staining, and in situs in general.

Marti Bosma's expertise in development are more removed from the academic content of this work, but her technical knowledge of imaging techniques, and her willingness to open her whole lab to me as I try new approaches has been deeply valued. In addition, she has probably shouldered more of my career and abstract academic worries than was her due, and again I am very thankful.

John Neumaier said of me, as I was rotating in his lab my first year here – that I was engaged intellectually, but that we would need to see whether that overlapped with being a good scientist. I have thought of this often, especially when I am trying to reframe or synthesis a new idea, and stuck spending hours tracking down a single citation. I worry that I tend towards being a dilettante, but John's psychiatrist gaze has kept me seeking good, detail-oriented, scientific balance, even when it is not directly on me. I thank him for his insight as much as for the time and expertise he has donated to me.

First after my mentor and advisory committee, I must thank Emma Morris. I shameless used a teaching assistantship in a physiology lab class to fish for a student assistant with able hands and with whom I got along. Emma turned out to be a great choice. I thank her for the countless hours of work, even on weekends, that she cheerily donated to the cause. I am proud to feel like I've shaped her view of science as she follows her career as a high-school science teacher. I knew of and celebrated her goal when she joined the lab, and I further thank her for her dedication to bettering public understanding, and to having the patience to keep debating with me the relative merits of different educational styles and venues.

Along the line of education, I would like to thank Eric Chudler. I have become involved in a great deal of community outreach for K-12 brain-focused education, and all of that has been possible thanks to Eric having laid the foundation, made relationships with local schools, and been willing to share his time and experience to help me and those who volunteered with me become an effective educational organization.

Finally I would like to thank the various people who have shaped my views, encouraged me, or just technically enabled me to do the work I've done. Phil Harding, Dr. Will Marrs, Dr. Mark Ellisman, Dr. Diana Price, Tom Deerinck, Yoshito Kosai, Billie Medina, and Drs. Michael Schwartz and Cheryl Wotus. Of course the real list of people to whom I owe thanks is much longer, but I hope they will not begrudge me cutting off the list here.